

Unified Optimization of Source Weights and Transfer Quantities in Multi-Source Transfer Learning: An Asymptotic Framework

Qingyue Zhang¹, Chang Chu¹, Haohao Fu¹, Tianren Peng¹, Yanru Wu¹, Guanbo Huang¹, Yang Li², and Shao-Lun Huang¹

Abstract—In multi-source transfer learning, a key challenge lies in how to appropriately differentiate and utilize heterogeneous source tasks. However, existing multi-source methods typically focus on optimizing either the source weights or the amount of transferred samples, largely neglecting their joint consideration. In this work, we propose a theoretical framework, Unified Optimization of Weights and Quantities (UOWQ), that jointly determines the optimal source weights and transfer quantities for each source task. Specifically, the framework formulates multi-source transfer learning as a parameter estimation problem based on an asymptotic analysis of a Kullback–Leibler divergence–based generalization error measure, leading to two main theoretical findings: 1) using all available source samples is always optimal when the weights are properly adjusted; 2) the optimal source weights are characterized by a principled optimization problem whose structure explicitly incorporates the Fisher information, parameter discrepancy, parameter dimensionality, and transfer quantities. Building on the theoretical results, we further propose a practical algorithm for multi-source transfer learning, and extend it to multi-task learning settings where each task simultaneously serves as both a source and a target. Extensive experiments on real-world benchmarks, including DomainNet and Office-Home, demonstrate that UOWQ consistently outperforms strong baselines. The results validate both the theoretical predictions and the practical effectiveness of our framework.

Index Terms—transfer learning, multi-source learning, asymptotic analysis, K-L divergence,

I. INTRODUCTION

Transfer learning has emerged as a critical paradigm in modern machine learning, especially in scenarios where labeled data is scarce for the target task [1]. By leveraging knowledge from related source tasks, transfer learning enables models to generalize more effectively and efficiently to the target task. In recent years, transfer learning has a wide range of applications. For example, in deep reinforcement learning, transfer learning plays a crucial role in accelerating

policy learning and improving sample efficiency by transferring policies, representations, or experience [2]. In healthcare, transfer learning leverages large medical datasets to support rare disease diagnosis with limited clinical data [3]. In natural language processing, pretrained models built on large-scale transfer learning foundations have revolutionized performance across a wide range of downstream tasks [4]. While single-source transfer learning has been studied earlier, growing attention is now being paid to multi-source transfer learning. With the rapid development of large language models (LLMs) trained on massive and diverse corpora, effectively leveraging complementary knowledge from multiple heterogeneous data sources has become increasingly important.

In multi-source transfer learning, how to differentially leverage multiple source tasks has emerged as a central research problem. From a statistical perspective, while incorporating additional data from source tasks can reduce estimation variance, sources that are overly dissimilar to the target task may introduce excessive systematic bias, outweighing the benefits of variance reduction. As a result, naive uniform transfer from multiple source tasks can lead to negative transfer [13], making the identification and effective utilization of truly related source tasks a key challenge. Existing approaches typically address this challenge from one of two separate perspectives. On one hand, **task- or source-weighting** methods aim to control the influence of different sources by assigning importance weights to source models or samples [9], [14], thereby mitigating bias caused by mismatched domains. In existing studies on task weighting, most frameworks implicitly assume that all source samples are utilized, while the transfer weights are determined independently of the transfer quantity. On the other hand, **sample selection** methods focus on determining the optimal transfer quantity for each source and identifying the source samples to be transferred [10]–[12]. Considering source weighting and transfer quantities in isolation restricts the solution space and can lead to suboptimal solutions, whereas jointly optimizing them leads to more principled and effective solutions. The goal of this work is to establish a unified theoretical framework that not only jointly determines the optimal source weights and transfer quantities, but also provides a principled interpretation of their interaction, thereby offering insights into existing weighting and sample selection strategies. In Table I, we provide a detailed comparison of the proposed method with several existing methods.

The authors are with the Tsinghua Shenzhen International Graduate School, Tsinghua University, Shenzhen, China. Yang Li is now with the School of Artificial Intelligence, The Chinese University of Hong Kong, Shenzhen, China. This work was done while she was with the Tsinghua Shenzhen International Graduate School, Tsinghua University, Shenzhen, China.

This work was supported in part by the National Key R&D Program of China under Grant 2021YFA0715202, the National Natural Science Foundation of China under Grants 62571296 and 62371270, and the Shenzhen Science and Technology Program under Grant KJZD20240903102700001.

Corresponding authors: Yang Li (yangl@cuhk.edu.cn), Shao-Lun Huang (tw2gold@gmail.com).

Our code is publicly available at: <https://github.com/zqy0126/UOWQ>.

TABLE I: **Comparison across matching-based transfer learning methods**, based on whether they perform quantity optimization, weight optimization, are tailored to multi-source, have task generality, have shot generality, and require target labels. The ‘✓’ represents obtaining the corresponding aspects, while ‘✗’ represents the opposite. Quantity optimization denotes the ability to determine how many source samples or data subsets should be transferred. Weight optimization denotes the ability to assign or learn weights for different source tasks or samples. Task generality denotes the ability to handle various target task types, and shot generality denotes the ability to avoid negative transfer in different target sample quantity settings, including few-shot and non-few-shot.

Method	Quantity Optimization	Weight Optimization	Multi-Source	Task Generality	Shot Generality	Target Label
MCW [5]	✗	✓	✓	✗	✗	Supervised
Leep [6]	✗	✗	✗	✓	✓	Supervised
Tong [7]	✗	✓	✓	✗	✓	Supervised
DATE [8]	✗	✓	✓	✓	✓	Unsupervised
H-ensemble [9]	✗	✓	✓	✗	✗	Supervised
FOMA [10]	✓	✗	✓	✗	✗	Supervised
DBF [11]	✓	✗	✗	✗	✗	Supervised
OTQMS [12]	✓	✗	✓	✓	✓	Supervised
UOWQ (Ours)	✓	✓	✓	✓	✓	Supervised

In this work, we develop a theoretical framework termed **Unified Optimization of Weights and Quantities (UOWQ)**, to determine the optimal weights and quantities for source tasks in transfer learning via asymptotic analysis. Through an asymptotic analysis of the measure based on Kullback–Leibler (K-L) divergence, we formulate the multi-source transfer learning problem as a parameter estimation problem, which in turn yields an optimization problem of the source weights and transfer quantities. First, we prove the conclusion that using all available source samples is always optimal once the weights are properly adjusted, and provide an intuitive interpretation of this result. Moreover, our analysis provides a closed-form solution for the optimal transfer weight in the single-source setting and characterizes the optimal weights in the multi-source setting via a convex optimization formulation, jointly accounting for the Fisher information, parameter discrepancy, parameter dimensionality, and transfer quantities. On this basis, we introduce practical algorithms capable of supporting both multi-source transfer learning and multi-task transfer learning. Finally, the effectiveness of the proposed algorithms is validated through experiments on real-world datasets.

The main contributions of this work are summarized as follows:

- **Theoretical framework.** We introduce UOWQ, a mathematical framework based on asymptotic analysis, to jointly optimize transfer quantities and source weights in multi-source transfer learning. Under joint optimization, we prove that using all available source samples is always optimal. In addition, we characterize the optimal transfer weights for each source via an optimization formulation that explicitly accounts for the transfer quantities.
- **Practical algorithm.** Based on our theory, we develop practical algorithms derived from the framework for both multi-source transfer learning and multi-task learning. Specifically, to cope with scarce target data and ensure robustness, the algorithms alternate between model optimization and source weight updates.
- **Experimental validation.** We perform extensive experiments on the `DomainNet` and `Office-Home` bench-

marks under both multi-source transfer learning and multi-task learning settings. In the 10-shot multi-source transfer scenario, UOWQ consistently outperforms strong baselines, achieving average accuracy improvements of 1.3% on `DomainNet` and 1.4% on `Office-Home`. Moreover, in the multi-task learning setting, UOWQ surpasses state-of-the-art task-weighting methods by 0.7% on `DomainNet` and 0.4% on `Office-Home` in terms of overall average performance. In addition, we conduct comprehensive ablation and robustness studies, including analyses under varying target-shot regimes, weight visualization, and computational efficiency evaluations, to further validate the theoretical insights and practical robustness of UOWQ.

This work is an extension of our previous conference paper [15], and the additional contributions are summarized as follows. First, the journal version presents a more explicit formulation for jointly optimizing transfer quantities and source weights, together with complete theoretical proofs. In addition, we provide further theoretical analysis, including an intuitive interpretation of why utilizing all source samples remains optimal under joint optimization in Section IV-B, as well as comparisons with related theoretical frameworks in Remark 4 and Table I. Second, in the practical algorithm part in Section V, we further develop a multi-task learning algorithm based on the proposed multi-source transfer learning algorithm. Finally, the experimental section is substantially strengthened with larger-scale datasets, more comprehensive baselines, and evaluations of the proposed multi-task learning extension, along with extensive analyses including ablation studies, weight visualization, robustness evaluation, computational efficiency analysis, and compatibility with Low-Rank Adaptation (LoRA).

The remainder of this paper is organized as follows. Section II reviews the related work. Section III introduces several preliminary results used in our analysis and presents the problem formulation. Section IV develops the main theoretical results to calculate the optimal source weights. Section V introduces practical algorithms. Section VI empirically evaluates

the proposed framework and validates the theoretical findings.

II. RELATED WORK

A. Multi-source Transfer Learning

Multi-source transfer learning (MSTL) leverages knowledge from multiple related source domains or tasks to improve performance on a target task, addressing challenges such as domain shift and negative transfer [16]–[18]. By emphasizing relevant sources while suppressing less informative ones, MSTL enhances generalization in heterogeneous settings, where effective learning requires balancing source contributions and mitigating distribution discrepancies.

From the perspective of the *transfer object*, multi-source transfer learning methods can be broadly categorized into **model-based** and **sample-based** transfer [19]. Model-based approaches leverage pretrained source models through fine-tuning or parameter adaptation [20], whereas sample-based methods jointly train on target and weighted source samples, enabling more direct exploitation of task-relevant source data [14], [21], [22].

From the perspective of the *transfer strategy*, existing methods can be further divided into **alignment-based** and **matching-based** approaches [23]. Alignment-based methods reduce domain discrepancy by explicitly aligning feature distributions [22], [24], [25], while matching-based methods emphasize informative sources or samples via selective weighting [7], [9], [14], [26]. Our method is more closely aligned with the **sample-based, matching-based** category, as it adopts a unified framework that jointly optimizes transfer quantities and source weights for weighted joint training.

B. Task weighting

Task weighting, also referred to as source weighting, is a representative class of **matching-based** approaches in multi-source transfer learning and multi-task learning, as it regulates the contribution of different tasks without explicitly aligning feature distributions. Its objective is to balance competing task objectives during joint optimization. Early approaches relied on **static weighting**, assigning fixed weights based on heuristics such as task priority or dataset size [27], but these methods lack adaptability to dynamic task interactions. Recent studies have therefore focused on **dynamic task weighting** strategies. For example, uncertainty-based weighting was introduced in [28], GradNorm balances tasks by normalizing gradient magnitudes [29], and DWA adjusts weights according to task learning speeds [30]. From a multi-objective optimization perspective, MGDA [31] formulates task weighting as a Pareto-optimal optimization problem.

Recent work has further extended task weighting to large-scale pretrained models, primarily through gradient-based matching mechanisms. For instance, task reweighting via gradient alignment has been studied in [32], while conflicting gradients are mitigated by CAGrad [33]. Other studies explore **meta-learning**-based strategies [34] and task affinity to automate weighting. Despite these advances, task weighting remains challenged by nonstationary task relationships [35],

scalability to large task sets, and the lack of strong theoretical guarantees [36], [37]. Benchmark datasets such as **Meta-Dataset** [38] have been introduced to facilitate standardized evaluation.

Most existing task-weighting methods operate at the model level, assigning scalar weights to source models in a mixture-of-experts fashion [39]. These approaches typically rely on task similarity [40], domain divergence [41], or validation performance [42]. In contrast, only a limited number of studies consider sample-level weighting, where source samples are reweighted and jointly trained with the target data in a unified framework [14], [21]. Moreover, most existing task-weighting methods implicitly assume access to all source samples, and the resulting weights are independent of the transfer quantity. While recent works have begun to study the problem of optimally selecting transferable source samples or transfer quantities [10]–[12], these efforts are largely decoupled from task-weight optimization. Our work provides a unified treatment that jointly optimizes task weights and transfer quantities, enabling principled control over both which sources to transfer from and how much to transfer.

C. Transfer Learning Theory

Existing theoretical studies in transfer learning can generally be divided into two primary categories. The first category aims to define and quantify the similarity or relatedness between source and target tasks. Numerous metrics have been proposed in this context, including the l_2 distance [43], optimal transport cost [44], LEEP (Log Expected Empirical Prediction) [6], Wasserstein distance [14], OTCE (Optimal Transport-based Conditional Entropy) [45], LogME [46], NCE [47], GBC (Geometric-Based Correlation) [48], and maximal correlation-based measures [5]. For example, LEEP [6] provides a probabilistic framework for transferability estimation by comparing model predictions on the target task. Meanwhile, OTCE [45] leverages optimal transport theory to quantify transferability under distribution shifts. These measures provide principled ways to assess how well knowledge from a source task can potentially benefit a target task.

This work belongs to the second group, which is dedicated to developing theoretical measures that assess and bound the generalization error in transfer learning scenarios. Various generalization error measures have been proposed to guide the assignment of task or source weights, including f -divergence [49], mutual information [50], \mathcal{H} -score [9], and \mathcal{X}^2 -divergence [7]. Specifically, the \mathcal{H} -score analytically characterizes the expected log-loss on the target task under a fixed source feature representation, thereby providing a principled basis for evaluating target predictive performance in transfer learning. Furthermore, a recently developed generalization measure based on K-L divergence [12] provides a rigorous foundation for determining optimal transfer quantities. In this work, we demonstrate that such a measure offers a more direct alignment with the cross-entropy loss—a standard objective in machine learning—than previous metrics. Consequently, we extend this metric and framework to jointly optimize source weights and transfer quantities.

III. PRELIMINARIES

In this section, we introduce the theoretical foundations of our framework. We first present the K-L divergence-based generalization error measure in Section III-A, which serves as the optimization objective. We then review the asymptotic normality of the MLE in Section III-B, which enables characterizing estimation variance. Finally, we formulate the multi-source transfer learning problem and its joint optimization objective in Section III-C.

A. K-L Divergence-Based Measure

We introduce a K-L divergence-based measure as the generalization error measure.

Definition 1 (The K-L divergence [51]). *The K-L divergence $D(P||Q)$ measures the difference between two probability distributions $P(X)$ and $Q(X)$ over the same probability space. It is defined as:*

$$D(P||Q) = \sum_{x \in \mathcal{X}} p(x) \log \frac{p(x)}{q(x)}.$$

In this work, we use the expectation of K-L divergence between the true distribution of target task $P_{X;\theta_0}$ and the distribution $P_{X;\hat{\theta}}$ learned from training samples as the generalization error measure, i.e.,

$$\mathbb{E} \left[D(P_{X;\theta_0} || P_{X;\hat{\theta}}) \right]. \quad (1)$$

Compared to other measures, the K-L divergence exhibits a closer correspondence with the generalization error measured by the cross-entropy loss; we formally justify this relationship in the Appendix.

B. Asymptotic Normality of the MLE

When attempting to recover the true parameter vector θ^* from independent and identically distributed (i.i.d.) observations generated according to the distribution $P_{X;\theta^*}$, we let \mathcal{D} denote a collection of n such i.i.d. samples. The maximum likelihood estimator (MLE) is then defined as the maximizer of the empirical log-likelihood:

$$\hat{\theta}_{\text{MLE}} = \arg \max_{\theta} \frac{1}{n} \sum_{x \in \mathcal{D}} \log P_{X;\theta}(x). \quad (2)$$

Provided that the underlying distribution satisfies the standard regularity assumptions, the MLE exhibits the well-known property of **asymptotic normality** [52]. Specifically, as the sample size increases, the distribution of the normalized estimation error converges in law to a multivariate Gaussian distribution:

$$\sqrt{n} \left(\hat{\theta}_{\text{MLE}} - \theta^* \right) \xrightarrow{d} \mathcal{N}(0, J(\theta^*)^{-1}), \quad (3)$$

where the notation “ -1 ” indicates the matrix inverse, and $J(\theta)$ denotes the Fisher information matrix [51]. The Fisher information matrix, which characterizes the amount of information carried by the distribution about the parameter, is defined as

$$J(\theta)^{d \times d} = \mathbb{E} \left[\left(\frac{\partial}{\partial \theta} \log P_{X;\theta} \right) \left(\frac{\partial}{\partial \theta} \log P_{X;\theta} \right)^T \right]. \quad (4)$$

Intuitively, the Fisher information matrix characterizes the local geometry of the log-likelihood function with respect to the parameter θ . It captures how sensitively the distribution responds to perturbations along different parameter directions, thereby reflecting the statistical identifiability of θ .

C. Problem Formulation

A multi-source transfer learning framework consists of a target task \mathcal{T} and multiple source tasks $\{\mathcal{S}_1, \dots, \mathcal{S}_K\}$ that provide auxiliary information to improve performance on \mathcal{T} . To generalize the analysis, we model \mathcal{T} as a parameter estimation problem governed by an underlying distribution $P_{X;\theta}$, where θ denotes the parameter of interest and X represents a generic random variable corresponding to the data. For example, in supervised learning, $X = (Z, Y)$ represents the joint distribution over input features Z and labels Y . The objective is to accurately estimate the true value of θ , which in deep learning corresponds to optimizing the network parameters of \mathcal{T} . Furthermore, we assume that the source tasks and the target task follow the same parametric model and share the same input space \mathcal{X} . For notational clarity, we present only the case where \mathcal{X} is discrete, while the theoretical results extend straightforwardly to continuous domains.

The target task \mathcal{T} has N_0 i.i.d. training samples drawn from $P_{X;\theta_0}$, where $\theta_0 \in \mathbb{R}^d$, and the training set is denoted by X^{N_0} . Similarly, each source task \mathcal{S}_i has N_i i.i.d. samples from $P_{X;\theta_i}$, where $i \in [1, K]$ and $\theta_i \in \mathbb{R}^d$, denoted by X^{N_i} . During training, each sample is weighted in the gradient descent procedure according to the source weight associated with its corresponding task. Motivated by this weighting mechanism, we formulate the training process as a parameter estimation problem and define the corresponding estimator. Specifically, $\hat{\theta}$ is denoted as the MLE based on the N_0 samples from \mathcal{T} and n_1, \dots, n_K samples from $\mathcal{S}_1, \dots, \mathcal{S}_K$ with weights w_1, \dots, w_K , where $n_i \in [0, N_i]$ and $w_i \in [0, +\infty]$, i.e.,

$$\hat{\theta} = \arg \max_{\theta} \sum_{x \in X^{N_0}} \log P_{X;\theta}(x) + \sum_{i=1}^K \sum_{x \in X^{n_i}} w_i \log P_{X;\theta}(x), \quad (5)$$

where we require $w_i \geq 0$ because negative weights would subtract sample likelihoods, contradict the statistical meaning of MLE and turn the weighted log-likelihood into a non-concave and unbounded objective.

In this work, our goal is to derive the optimal transfer weight w_1^*, \dots, w_K^* and transfer quantities n_1^*, \dots, n_K^* of source tasks $\mathcal{S}_1, \dots, \mathcal{S}_K$ to minimize the K-L based measure between the true distribution of target task $P_{X;\theta_0}$ and the distribution $P_{X;\hat{\theta}}$ learned from training samples, i.e.,

$$w_1^*, \dots, w_K^*, n_1^*, \dots, n_K^* = \arg \min_{w_1, \dots, w_K, n_1, \dots, n_K} \mathbb{E} \left[D(P_{X;\theta_0} || P_{X;\hat{\theta}}) \right]. \quad (6)$$

For theoretical analysis, we assume a compact parameter space Θ and standard regularity conditions on $P_{X;\theta}$, including differentiability, parameter-independent support, and finite, positive Fisher information.

IV. THEORETICAL CHARACTERIZATION OF OPTIMAL SOURCE WEIGHTS AND TRANSFER QUANTITIES

In this section, we present the main theoretical results of UOWQ. We first characterize the optimal transfer quantity and the optimal source weight in the single-source setting, deriving closed-form expressions in Section IV-A. We then extend the analysis to the multi-source setting, where the joint optimization problem admits a convex formulation and a tractable numerical solution in Section IV-B.

A. Single-Source Transfer Learning

In this subsection, we first analyze the case where the parameter is one-dimensional in Theorem 2. We then extend the method to the high-dimensional setting in Proposition 3. Throughout this paper, we denote scalar-valued parameters by θ and high-dimensional parameters by $\underline{\theta}$. In analyzing the target parameter estimation problem, directly computing the K-L measure is intractable in general. Therefore, we conduct our analysis primarily in the asymptotic regime, where the behavior of the estimator becomes more tractable. To begin with, we consider the transfer learning scenario where we have one target task \mathcal{T} with N_0 training samples and one source task \mathcal{S}_1 with N_1 training samples. In this case, we aim to determine the optimal transfer quantity $n_1^* \in [1, N_1]$ and the optimal transfer weight $w_1^* \in [0, +\infty]$. To facilitate our mathematical derivations, we assume N_0 and N_1 are asymptotically comparable, and the distance between the parameters of the target task and source task is sufficiently small (*i.e.*, $|\theta_0 - \theta_1| = O(\frac{1}{\sqrt{N_0}})$). Considering the similarity of low-level features among tasks of the same type [53], this assumption is made without loss of generality, and similar assumptions have also been adopted in the prior literature [12].

Theorem 2. (proved in the Appendix) *In the single-source setting with 1-dimensional models $P_{X;\theta_0}$ and $P_{X;\theta_1}$, we assume that $\theta_0, \theta_1 \in \mathbb{R}$ and $|\theta_0 - \theta_1| = O(\frac{1}{\sqrt{N_0}})$. Then, the K-L measure $\mathbb{E}[D(P_{X;\underline{\theta}_0} || P_{X;\underline{\theta}})]$ can be expressed as:*

$$\frac{1}{2} \left(\underbrace{\frac{N_0 + w_1^2 n_1}{(N_0 + w_1 n_1)^2}}_{\text{variance term}} + \underbrace{\frac{w_1^2 n_1^2}{(N_0 + w_1 n_1)^2} t}_{\text{bias term}} \right) + o\left(\frac{1}{N_0}\right), \quad (7)$$

where

$$t \triangleq J(\theta_0) (\theta_1 - \theta_0)^2. \quad (8)$$

For **optimal transfer quantity**, by minimizing the above expression, we obtain that maximizing the transfer quantity is optimal, *i.e.*,

$$n_1^* = N_1. \quad (9)$$

Moreover, the solution of **optimal transfer weight** w_1^* is

$$w_1^* = \frac{1}{1 + tN_1}. \quad (10)$$

In Fig. 1, we provide an intuitive explanation for the existence of the optimal weight w_1^* defined in (10). We now discuss several properties of the optimal weight w_1^* . We observe that as the distance between θ_0 and θ_1 increases,

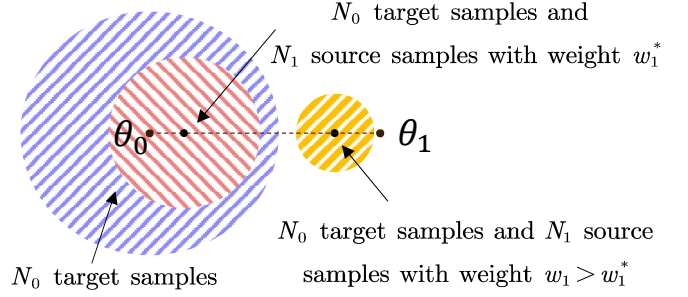


Fig. 1: The three circles represent the errors corresponding to transfer weight $w_1 = 0$, $w_1 = w_1^*$, and $w_1 > w_1^*$. The distance from each circle's center to θ_0 represents the bias of estimation, and the radius represents the variance. As the transfer weight of source increases, the bias term increases, while the variance term decreases for $w_1 \in [0, 1]$ and increases for $w_1 \in (1, +\infty)$. The optimal w_1^* achieves the best trade-off between them.

t increases and w_1^* decreases accordingly. In particular, as $|\theta_0 - \theta_1| \rightarrow 0$, w_1^* approaches one, whereas as the discrepancy becomes sufficiently large, w_1^* approaches zero. This shows that the weighting strategy reduces the influence of the source domain when it exhibits substantial discrepancies from the target. Moreover, as the quantity of source samples N_1 increases, w_1^* also decreases. This illustrates that the derived weight adaptively controls the trade-off between the target and source information, preventing the source from dominating even when it is abundant.

In the following, we extend the result of Theorem 2 to the high-dimensional setting.

Proposition 3. (proved in the Appendix) *In the single-source setting with d -dimensional models $P_{X;\underline{\theta}_0}$ and $P_{X;\underline{\theta}_1}$, we assume that $\underline{\theta}_0, \underline{\theta}_1 \in \mathbb{R}^d$ and $\|\underline{\theta}_0 - \underline{\theta}_1\| = O(\frac{1}{\sqrt{N_0}})$. Then, the K-L measure takes the following form:*

$$\frac{d}{2} \left(\frac{N_0 + w_1^2 n_1}{(N_0 + w_1 n_1)^2} + \frac{w_1^2 n_1^2}{(N_0 + w_1 n_1)^2} t \right) + o\left(\frac{1}{N_0}\right), \quad (11)$$

where

$$t \triangleq \frac{(\underline{\theta}_1 - \underline{\theta}_0)^\top J(\underline{\theta}_0) (\underline{\theta}_1 - \underline{\theta}_0)}{d}. \quad (12)$$

Here, t is a scalar, $J(\underline{\theta}_0) \in \mathbb{R}^{d \times d}$ denotes the Fisher information matrix evaluated at $\underline{\theta}_0$, and $(\underline{\theta}_1 - \underline{\theta}_0) \in \mathbb{R}^d$ is the coordinate-wise difference between the two parameter vectors. Finally, the **optimal transfer quantity** is the same form as (9) and the **optimal transfer weight** w_1^* is the same form as (10).

Compared with Theorem 2, Proposition 3 retains an analogous structural form in its mathematical expression. This structural resemblance enables us to follow a conceptually similar analytical route to determine the corresponding optimal quantity of knowledge transfer. It is worth emphasizing that the appearance of the Fisher information matrix J in the t -term is a direct consequence of the theoretical derivation, rather than a modeling choice or an explicitly imposed mechanism. The

resulting expression admits a clear interpretation: the Fisher information matrix implicitly induces a dimension-weighted aggregation over parameter directions, where the contribution of each direction is determined by the sensitivity of the likelihood. Parameter directions along which the likelihood is more sensitive to perturbations contribute more prominently to the derived measure, while directions with lower sensitivity have a reduced influence.

In addition, a closer inspection of Equation (11) reveals that the associated K-L measure exhibits a growth trend as the parameter dimensionality d increases. From a practical perspective, this scaling trend indicates that as models grow in complexity—characterized by increasingly large parameter spaces—the learning process becomes more intricate, thereby amplifying the challenge of achieving effective knowledge transfer. This observation is consistent with established findings in the literature [7], which indicate that increasing model complexity inherently exacerbates the difficulty of cross-task generalization.

Remark 4 (Connection to Prior Work). *The expression in Theorem 2 and Proposition 3 coincides with the results obtained by [7]. Equation (5) can be transformed to*

$$\begin{aligned} \hat{\theta} &= \arg \max_{\theta} \frac{\sum_{x \in X^{N_0}} \log P_{X;\theta}(x) + \sum_{x \in X^{N_1}} w_1 \log P_{X;\theta}(x)}{N_0 + w_1 N_1}, \\ &= \arg \max_{\theta} \mathbb{E}_{\hat{P}_{\text{mix}}} [\log P_{X;\theta}(x)], \end{aligned} \quad (13)$$

where

$$\hat{P}_{\text{mix}} := \frac{N_0}{N_0 + w_1 N_1} \hat{P}(X_0^{N_0}) + \frac{w_1 N_1}{N_0 + w_1 N_1} \hat{P}(X_1^{N_1}). \quad (14)$$

Substituting the optimal weight (10) into (14), we have

$$\hat{P}_{\text{mix}} := \frac{t + \frac{1}{N_1}}{t + \frac{1}{N_0} + \frac{1}{N_1}} \hat{P}(X_0^N) + \frac{\frac{1}{N_0}}{t + \frac{1}{N_0} + \frac{1}{N_1}} \hat{P}(X_1^N). \quad (15)$$

This formulation exhibits a notable similarity to the conclusions in [7]. In particular, both frameworks contain terms that scale with the inverse of the transfer quantities, highlighting the importance of accounting for sample size when determining the transfer weights. However, our framework differs from their work not only in the weighting mechanism but also in the treatment of model discrepancy and dimensionality. Specifically, Tong et al. [7] adopt a model-based weighting strategy, whereas our approach employs a sample-based weighting scheme. Their analysis quantifies task similarity via a χ^2 -distance, while the discrepancy term t in our formulation measures model distance directly in the parameter space and incorporates model complexity through Fisher information. Moreover, parameter dimensionality enters the weighting mechanism differently in the two approaches.

B. Multi-Source Transfer Learning

In this subsection, we first present the expression of the K-L measure in the multi-source setting, as stated in Theorem 5. By minimizing this expression, we derive a method to compute the optimal source weights and analyze its computational

complexity. Moreover, we provide an interpretation of the theoretical result that using all available samples is optimal when the weights are adjustable.

Theorem 5. (proved in the Appendix) *In the multi-source setting with d -dimensional models $P_{X;\theta_0}$ for the target task and $P_{X;\theta_i}$, $i \in [1, K]$ for the source tasks, we assume that $\theta_0, \theta_1 \dots \theta_K \in \mathbb{R}^d$ and $\|\theta_0 - \theta_i\| = O(\frac{1}{\sqrt{N_0}})$. Then, the K-L measure is given by*

$$\frac{d}{2} \left(\frac{N_0}{(N_0 + s)^2} + \frac{s^2}{(N_0 + s)^2 t} \right) + o\left(\frac{1}{N_0}\right), \quad (16)$$

where we denote $b_i = n_i w_i$, $s = \sum_{i=1}^K b_i$, $\alpha_i = \frac{b_i}{s}$, and

$$t = \frac{\underline{\alpha}^T \left(\text{diag} \left(\frac{d}{n_1}, \dots, \frac{d}{n_K} \right) + \Theta^T J(\theta_0) \Theta \right) \underline{\alpha}}{d}. \quad (17)$$

In (17), $\underline{\alpha} = [\alpha_1, \dots, \alpha_K]^T$ is a K -dimensional vector, and

$$\Theta^{d \times K} = [\theta_1 - \theta_0, \dots, \theta_K - \theta_0]. \quad (18)$$

For optimal transfer quantities, by minimizing (16), we obtain that maximizing the transfer quantities is optimal, i.e., $n_i^ = N_i$. Moreover, we propose a method to compute the optimal source weights, which will be elaborated in the following paragraph.*

We next present the method to compute the optimal value of w_i to minimize (16). The minimization problem is

$$(s^*, \underline{\alpha}^*) \leftarrow \arg \min_{(s, \underline{\alpha})} \frac{d}{2} \left(\frac{N_0}{(N_0 + s)^2} + \frac{s^2}{(N_0 + s)^2 t} \right) + o\left(\frac{1}{N_0}\right). \quad (19)$$

We reformulate this optimization problem as a sequential optimization process, and explicitly formulate the constraints as follows.

$$\begin{aligned} (s^*, \underline{\alpha}^*) &\leftarrow \arg \min_{s \in [0, +\infty]} \frac{d}{2} \left(\frac{N_0}{(N_0 + s)^2} + \frac{s^2}{(N_0 + s)^2} \right), \quad (20) \\ &\arg \min_{\underline{\alpha} \in \mathcal{A}} \frac{\underline{\alpha}^T \left(\text{diag} \left(\frac{d}{N_1}, \dots, \frac{d}{N_K} \right) + \Theta^T J(\theta_0) \Theta \right) \underline{\alpha}}{d}, \quad (21) \end{aligned}$$

where

$$\mathcal{A} = \left\{ \underline{\alpha} \mid \sum_{i=1}^K \alpha_i = 1, \alpha_i \geq 0, i = 1, \dots, K \right\}. \quad (22)$$

This problem requires optimizing the objective function over two variables: a scalar variable s representing the total weighted transfer quantity, and a vector variable $\underline{\alpha}$ representing the proportion of each source domain in s . First, we compute the optimal $\underline{\alpha}^* = [\alpha_1^*, \dots, \alpha_K^*]^T$ under the constraint \mathcal{A} to minimize t , which is a $K \times K$ non-negative quadratic programming problem with respect to $\underline{\alpha}$, i.e.,

$$\underline{\alpha}^* = \arg \min_{\underline{\alpha} \in \mathcal{A}} \underline{\alpha}^T \frac{\left(\text{diag} \left(\frac{d}{N_1}, \dots, \frac{d}{N_K} \right) + \Theta^T J(\underline{\theta}_0) \Theta \right)}{d} \underline{\alpha}. \quad (23)$$

In the quadratic coefficient matrix of this optimization problem, the first component, $\text{diag} \left(\frac{d}{N_1}, \dots, \frac{d}{N_K} \right)$, is diagonal and therefore strictly positive definite. The second component, $\Theta^T J(\underline{\theta}_0) \Theta$, is positive semi-definite since the Fisher information matrix $J(\underline{\theta}_0)$ is positive definite by the assumptions in Section III. Consequently, the sum of these two components is positive definite, which guarantees that the optimization problem is convex and admits a unique global optimum. By this procedure, we obtain t^* and $\underline{\alpha}^*$ that minimize t . Then we get the optimal value of s , which is always

$$s^* = \frac{1}{t^*}. \quad (24)$$

Finally, we use optimal s^* and $\underline{\alpha}_i^*$ to get the optimal weights by

$$w_i^* = \frac{s^* \alpha_i^*}{N_i}. \quad (25)$$

The time complexity of this optimization is dominated by solving a $K \times K$ quadratic programming problem over $\underline{\alpha}$, which can be solved in $\mathcal{O}(K^3)$ time using a primal-dual interior-point solver. In most standard transfer learning benchmarks, the number of available source domains is modest (typically $K \leq 10$), rendering the $\mathcal{O}(K^3)$ computational complexity manageable for real-world applications. For cases where the number of available source domains is substantially larger, one feasible strategy to preserve scalability is to perform a preliminary clustering or aggregation of domains with high similarity before executing our algorithm.

Moreover, the finding that maximizing the transfer quantity is optimal is non-trivial and theoretically insightful. Conventional wisdom in transfer learning holds that excessive use of source data without controlling domain discrepancy can amplify bias and cause negative transfer [54]. This perspective has motivated many approaches that either down-weight or selectively discard source samples to mitigate distribution mismatch [10]–[12]. On the other hand, some methods by default exploit all source data for joint training, often relying on heuristic weighting. Our framework provides a new theoretical perspective by jointly optimizing transfer quantity and source weights. Through asymptotic analysis, we prove that when weights are allowed to adjust, the optimal solution always employs all available source samples. The key insight is that enlarging the effective sample size strictly reduces variance, while the weighting mechanism simultaneously suppresses the bias introduced by heterogeneous domains. This dual effect reconciles prior intuitions: discarding data may reduce bias but weakens variance reduction, while our analysis shows that full data utilization with proper weighting achieves a better bias–variance trade-off. Consequently, our analysis offers a principled justification for exploiting all source data in multi-source transfer learning.

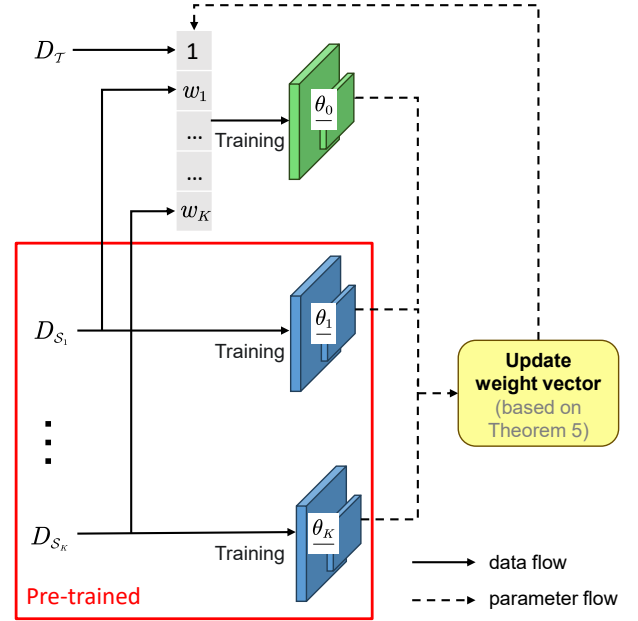


Fig. 2: **Overview of the UOWQ training pipeline:** At each iteration, the model parameters are optimized via gradient descent using target data together with weighted samples from each source task. The source weights are subsequently updated based on the current model parameters. This alternating optimization procedure establishes an iterative feedback loop that jointly updates the source weights and the target model.

V. PRACTICAL ALGORITHMS

In this section, we introduce practical algorithms derived from our theory for multi-source transfer learning and multi-task learning. Specifically, we propose practical algorithms of UOWQ for multi-source transfer learning in Algorithm 1 and for multi-task learning in Algorithm 2.

Firstly, we focus on Algorithm 1 to illustrate the proposed approach, whose overall workflow is shown in Fig. 2. In UOWQ, when computing the optimal source weights based on Theorem 5, we use the parameters of pretrained source models to replace $\underline{\theta}_1, \dots, \underline{\theta}_K$. Considering that the source model can be trained using sufficient labeled data, it is reasonable to use the learned parameters as a good approximation of the true underlying parameters. In contrast, the amount of target data in transfer learning is often insufficient, so it is difficult to accurately estimate the true parameter $\underline{\theta}_0$ - the parameter of the target task model - using only the target data. Therefore, as shown in lines 5-12 of Algorithm 1, we adopt a **dynamic weight update strategy**. Specifically, in the first epoch, we train $\underline{\theta}_0$ with the source weights initialized to zero, which is equivalent to using only the target data. This $\underline{\theta}_0$ is then used, along with Theorem 5, to determine the optimal source weight for each source task. Thereafter, training proceeds in an alternating manner: given the current weights, we update $\underline{\theta}_0$, and given the updated model, we recompute the weights. This process is repeated at each epoch, enabling iterative refinement of both the model and the weights. Such an iterative scheme allows adaptive weight adjustment, resulting in more stable

optimization and improved transfer performance. In particular, the loss function ℓ is the negative log-likelihood. Moreover, in line 9, we compute the matrix J using the widely adopted **empirical Fisher** approach in deep learning [55], [56].

We further extend the proposed framework to the multi-task learning setting, where each task simultaneously serves as both a target and a source for the others, and the objective is to learn task-specific models for all tasks. Suppose we are given K tasks $\{S_k\}_{k=1}^K$, where each task S_k is associated with dataset D_{S_k} and parameter θ_k . When optimizing task k , we treat S_k as the target task and the remaining tasks $\{S_{k'}\}_{k' \neq k}$ as auxiliary sources, and we construct its training set by combining all samples from the target task with the weighted samples from the remaining tasks, where the weights $w_{k'}^{(k)}$ are computed by UOWQ. The resulting problem becomes a joint optimization over all task parameters $\{\theta_k\}_{k=1}^K$, leading to an alternating optimization procedure between tasks, summarized in Algorithm 2.

VI. EXPERIMENTS

A. Experimental Settings

In the experiments, we evaluated the practical algorithms of UOWQ in real-world datasets. In particular, we evaluated Algorithm 1 in the multi-source transfer learning setting and Algorithm 2 in the multi-task learning setting.

Benchmark Datasets. The Office-Home dataset [57] consists of four domains: Art (**Ar**, 2,427 samples), Clipart (**Cl**, 4,365 samples), Product (**Pr**, 4,439 samples), and Real World (**Rw**, 4,357 samples). Each domain contains images from the same 65 object categories, resulting in a total of 15,588 samples. The DomainNet dataset [58] comprises six distinct domains: Clipart (**Cl**, 48,841 samples), Infograph (**In**, 48,466 samples), Painting (**Pa**, 48,529 samples), Quickdraw (**Qd**, 48,755 samples), Real (**Re**, 120,906 samples), and Sketch (**Sk**, 49,044 samples). Each domain includes images from the same 345 object categories, yielding a total of 364,541 samples. Data examples of the two datasets are shown in Fig. 3. We treat the multi-class classification problem on each domain as an individual task.

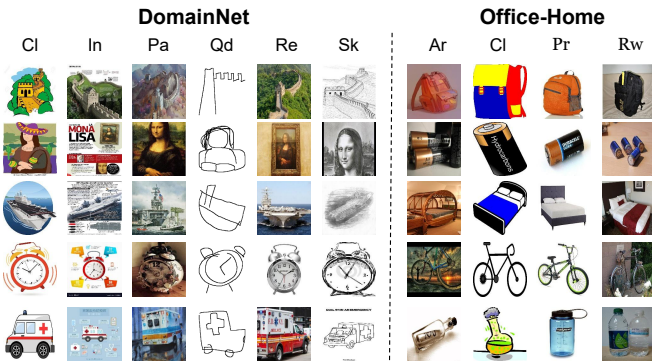


Fig. 3: **Overview of the Datasets:** Examples from the cross-domain datasets DomainNet and Office-Home, where images from different domains exhibit distinct visual styles or are captured using different devices.

Algorithm 1 UOWQ for Multi-Source Transfer Learning

- 1: **Input:** Target data $D_{\mathcal{T}} = \{(z_{\mathcal{T}}^j, y_{\mathcal{T}}^j)\}_{j=1}^{N_0}$, source data $\{D_{S_k} = \{(z_{S_k}^j, y_{S_k}^j)\}_{j=1}^{N_k}\}_{k=1}^K$, model type f_{θ} and its parameters θ_0 for target task and $\{\theta_k\}_{k=1}^K$ for source tasks, parameter dimension d , source weights $\{w_k\}_{k=1}^K$
// z represents the feature and y represents the label
- 2: **Parameter:** Learning rate η .
- 3: **Initialize:** randomly initialize θ_0 , use parameters of pre-trained source models to initialize $\{\theta_k\}_{k=1}^K$, initialize weights $\{w_k\}_{k=1}^K = 0$
- 4: **Output:** a well-trained θ_0 for target task model f_{θ_0}
- 5: **repeat**
- 6:
$$\mathcal{L}_{train} \leftarrow \frac{\sum_{(z^j, y^j) \in D_{\mathcal{T}}} \ell(y^j, f_{\theta_0}(z^j))}{|D_{\mathcal{T}} \cup \{D_{S_k}\}_{k=1}^K|} + \frac{\sum_{k=1}^K \sum_{(z^j, y^j) \in D_{S_k}} \ell(y^j, f_{\theta_0}(z^j)) * w_k}{|D_{\mathcal{T}} \cup \{D_{S_k}\}_{k=1}^K|}$$
- 7: $\theta_0 \leftarrow \theta_0 - \eta \nabla_{\theta_0} \mathcal{L}_{train}$
- 8: $\Theta \leftarrow [\theta_1 - \theta_0, \dots, \theta_K - \theta_0]^T$
- 9:
$$J(\theta_0) \leftarrow \frac{\sum_{(z^j, y^j) \in D_{\mathcal{T}}} \nabla_{\theta_0} \ell(y^j, f_{\theta_0}(z^j)) (\nabla_{\theta_0} \ell(y^j, f_{\theta_0}(z^j)))^T}{|D_{\mathcal{T}}|}$$
- 10: $(s^*, \underline{\alpha}^*) \leftarrow \arg \min_{(s, \underline{\alpha})} \frac{d}{2} \left(\frac{N_0}{(N_0+s)^2} + \frac{s^2}{(N_0+s)^2} t \right)$
- 11: $w_k^* \leftarrow \frac{s^* \alpha_k^*}{N_k}, k = 1, \dots, K$
- 12: **until** θ_0 converges;

Algorithm 2 UOWQ for Multi-Task Learning

- 1: **Input:** Datasets $\{D_{S_k} = \{(z_{S_k}^j, y_{S_k}^j)\}_{j=1}^{N_k}\}_{k=1}^K$, model type f_{θ} , parameters $\{\theta_k\}_{k=1}^K$, parameter dimension d , weights $\{w_{k'}^{(k)}\}_{k, k'=1, k' \neq k}^K$
- 2: **Parameter:** Learning rate η
- 3: **Initialize:** Randomly initialize $\{\theta_k\}_{k=1}^K$, set weights $w_{k'}^{(k)} = 0$ for all $k' \neq k$
- 4: **Output:** well-trained parameters $\{\theta_k\}_{k=1}^K$
- 5: **repeat**
- 6: **for** each $k = 1$ to K **do**
- 7:
$$\mathcal{L}_{train}^{(k)} \leftarrow \frac{\sum_{(z^j, y^j) \in D_{S_k}} \ell(y^j, f_{\theta_k}(z^j))}{|\{D_{S_k}\}_{k=1}^K|} + \frac{\sum_{k' \neq k} \sum_{(z^j, y^j) \in D_{S_{k'}}} \ell(y^j, f_{\theta_{k'}}(z^j)) * w_{k'}^{(k)}}{|\{D_{S_k}\}_{k=1}^K|}$$
- 8: $\theta_k \leftarrow \theta_k - \eta \nabla_{\theta_k} \mathcal{L}_{train}^{(k)}$
- 9: $\Theta^{(k)} \leftarrow \left[\theta_1 - \theta_k, \dots, \theta_{k-1} - \theta_k, \theta_{k+1} - \theta_k, \dots, \theta_K - \theta_k \right]^T$
- 10:
$$J^{(k)} \leftarrow \frac{\sum_{(z^j, y^j) \in D_{S_k}} \nabla_{\theta_k} \ell(y^j, f_{\theta_k}(z^j)) (\nabla_{\theta_k} \ell(y^j, f_{\theta_k}(z^j)))^T}{|D_{S_k}|}$$
- 11: $(s_k^*, \underline{\alpha}^{*(k)}) \leftarrow \arg \min_{(s, \underline{\alpha})} \frac{d}{2} \left(\frac{N_k}{(N_k+s)^2} + \frac{s^2}{(N_k+s)^2} t \right)$
- 12: $w_{k'}^{(k)} \leftarrow \frac{s_k^* \alpha_{k'}^{*(k)}}{N_{k'}}, \forall k' \neq k$
- 13: **end for**
- 14: **until** all θ_k converge

In the multi-source transfer learning setting, our goal is to transfer useful knowledge from multiple source domains to a specific target domain. In the experiments under this setting, our evaluation is performed in the **supervised-10-shot** learning setting, where only 10 labeled samples per class are available in the target domain, while all available samples from the source domains in the dataset are utilized.

In the multi-task learning setting, each task simultaneously serves as both a target task to be learned and a source task from which knowledge is transferred to other tasks. In the experiments under this setting, all available data from every domain in the dataset are fully utilized.

Implementation Details. Experiments are conducted on NVIDIA A800 GPU. To ensure fair comparison with prior work, different configurations are adopted for two scenarios. For the multi-source transfer learning setting, we adopt ViT-Small [59] pre-trained on ImageNet-21k [60] as the backbone and Adam optimizer [61] with a learning rate of 10^{-5} . We allocate 20% of the dataset as the test set and report the best accuracy within 5 epochs of early stopping. For the multi-task learning setting, we use ResNet-18 [62] pre-trained on ImageNet-1k [63] as the backbone and Adam optimizer with a learning rate of 10^{-4} . The dataset is randomly divided into 60% for training, 20% for validation, and 20% for testing.

B. Experimental Design and Model Adaptation

Baselines. We compare our method with several SOTA methods in both settings.

For the multi-source transfer learning setting, we follow a unified evaluation setup for all methods. The baselines include: 1) Source Ablation Studies: Target-Only, Single-Source-Avg/Single-Source-Best (average/best single-source transfer results), AllSources \cup Target (transfer results using all available source data without weighting). 2) Model-Weighting Based Few-Shot Methods: H-ensemble [9], MCW [5]. 3) Sample-Based Few-Shot Methods: MADA [21], WADN [14], OTQMS [12]. Furthermore, we report the results of several unsupervised methods for reference, including MSFDA [64], DATE [8], M3SDA [58]. For these unsupervised methods, we adopt a different experimental setting: instead of following the supervised-10-shot setting, we utilize all available unlabeled target data, corresponding to an unsupervised-all-shot setting.

For the multi-task learning setting, we follow the same experimental setup as in [68] and compare with the baselines reported in their work. The baselines include: Equal Weighting (EW), MGDA-UB [31], GradNorm [29], PCGrad [65], CAGrad [33], RGW [66], MoCo [67], and MoDo [68].

C. Few-Shot Multi-Source Transfer Performance

We evaluated our method, UOWQ, against the baseline methods using the Office-Home and the DomainNet datasets. The quantitative results for the multi-source transfer learning setting are summarized in Table II. We make the following observations:

Overall Performance. In general, compared to the other baselines, UOWQ achieves the best performance. Specifically,

in the multi-source transfer learning setting, UOWQ outperforms the state-of-the-art (OTQMS) by an average of 1.3% on DomainNet and 1.4% on Office-Home.

Sample-Based vs. Model-Based. In the multi-source transfer learning setting, methods based on sample consistently exhibit stronger performance than those relying on model-level aggregation. Specifically, approaches that directly optimize a mixture of source and target samples—such as WADN, MADA, OTQMS, and UOWQ—tend to outperform model-based techniques like H-ensemble and MCW, which combine predictions or parameters from multiple pretrained models. A plausible explanation is that sample-based strategies allow the target model to interact directly with source data during training, enabling more flexible adaptation to target-specific distributions, whereas model-based methods are constrained by fixed source representations.

Unified Optimization Outperforms Isolated Optimization. Among sample-based approaches, UOWQ further improves upon existing baselines by jointly optimizing both the transfer quantities and the corresponding weights, while also deriving transfer weights that are explicitly dependent on the transfer quantities. In contrast, OTQMS focuses solely on optimizing transfer quantities, whereas WADN primarily adjusts weighting coefficients.

Effectiveness of Limited Supervision. We further compare supervised and unsupervised multi-source transfer learning approaches under otherwise identical settings. As shown in Table II, even when unsupervised methods such as MSFDA and M3SDA leverage all available target samples—up to 1.3×10^5 instances in the Real domain of DomainNet—their performance remains inferior to supervised methods that utilize only a small number of labeled target samples (3450 in total). This comparison suggests that a modest amount of target supervision can provide substantially more informative guidance than large quantities of unlabeled data, underscoring the practical value of few-shot supervision in multi-source transfer learning.

Gains over Strong Baselines in Challenging Domains. Beyond average accuracy improvements, UOWQ consistently outperforms strong baselines in the most challenging domains. For example, in the DomainNet experiments, UOWQ improves over the previous best results in the Quickdraw target domain by 3.0% absolute accuracy (36.8% vs. 33.8%) and in the Infograph target domain by 1.4% (35.2% vs. 33.8%). These gains in visually divergent domains demonstrate that UOWQ’s sample-weighting strategy is particularly effective in mitigating domain shift. These results highlight the robustness of UOWQ under severe domain shifts, where knowledge transfer is particularly challenging.

D. Multi-Task Learning Performance

The results for the multi-task learning setting are summarized in Table III. We make the following observations.

Overall Performance Superiority. Across both benchmarks, UOWQ achieves the best overall average performance. On DomainNet, it obtains the highest mean accuracy of 51.9%, improving upon the strongest baseline MoDo (51.2%)

TABLE II: **Multi-Source Transfer Performance on DomainNet and Office-Home.** The arrows indicate transferring from the rest tasks. The highest/second-highest accuracy is marked in Bold/Underscore form respectively.

Method	Backbone	DomainNet							Office-Home				
		→C	→I	→P	→Q	→R	→S	Avg	→Ar	→Cl	→Pr	→Rw	Avg
Unsupervised-all-shots													
MSFDA [64]	ResNet50	66.5	21.6	56.7	20.4	70.5	54.4	48.4	75.6	62.8	84.8	85.3	77.1
DATE [8]	ResNet50	-	-	-	-	-	-	-	75.2	60.9	<u>85.2</u>	84.0	76.3
M3SDA [58]	ResNet101	57.2	24.2	51.6	5.2	61.6	49.6	41.5	-	-	-	-	-
Supervised-10-shots													
<i>Source-Ablation Methods:</i>													
Target-Only	ViT-S	14.2	3.3	23.2	7.2	41.4	10.6	16.7	40.0	33.3	54.9	52.6	45.2
Single-Source-Avg	ViT-S	50.4	22.1	44.9	24.7	58.8	42.5	40.6	65.2	53.3	74.4	72.7	66.4
Single-Source-Best	ViT-S	60.2	28.0	55.4	28.4	66.0	49.7	48.0	72.9	60.9	80.7	74.8	72.3
AllSources \cup Target	ViT-S	71.7	32.4	60.0	31.4	71.7	58.5	54.3	77.0	62.3	84.9	84.5	77.2
<i>Model-Weighting Based Few-Shot Methods:</i>													
MCW [5]	ViT-S	54.9	21.0	53.6	20.4	70.8	42.4	43.9	68.9	48.0	77.4	<u>86.0</u>	70.1
H-ensemble [9]	ViT-S	53.4	21.3	54.4	19.0	70.4	44.0	43.8	71.8	47.5	77.6	79.1	69.0
<i>Sample-Based Few-Shot Methods:</i>													
WADN [14]	ViT-S	68.0	29.7	59.1	16.8	<u>74.2</u>	55.1	50.5	60.3	39.7	66.2	68.7	58.7
MADA [21]	ViT-S	51.0	12.8	60.3	15.0	81.4	22.7	40.5	<u>78.4</u>	58.3	82.3	85.2	76.1
OTQMS	ViT-S	<u>72.8</u>	<u>33.8</u>	<u>61.2</u>	<u>33.8</u>	73.2	<u>59.8</u>	<u>55.8</u>	78.1	<u>64.5</u>	<u>85.2</u>	84.9	<u>78.2</u>
UOWQ	ViT-S	74.5	35.2	61.8	36.8	73.3	60.9	57.1	78.7	65.1	86.9	87.6	79.6

TABLE III: **Multi-Task Learning Performance on DomainNet and Office-Home.** Each column indicates the target domain used for evaluation. The highest and second-highest accuracy are marked in **bold** and underline, respectively.

Method	DomainNet							Office-Home				
	C	I	P	Q	R	S	Avg	Ar	Cl	Pr	Rw	Avg
EW	67.3	22.7	<u>56.1</u>	35.1	69.3	55.9	51.1	63.0	76.5	88.5	77.7	76.4
MGDA-UB [31]	69.0	22.4	<u>56.1</u>	31.7	69.7	55.9	50.8	64.3	75.3	<u>89.7</u>	79.3	77.2
GradNorm [29]	67.1	<u>22.5</u>	<u>56.1</u>	35.7	69.3	55.8	51.1	65.5	75.3	<u>88.7</u>	78.9	77.1
PCGrad [65]	67.8	22.7	56.0	34.7	69.2	56.1	51.1	63.9	76.0	88.9	78.3	76.8
CAGrad [33]	<u>68.4</u>	22.7	55.7	32.1	<u>69.8</u>	55.6	50.7	63.8	75.9	89.1	78.3	76.8
RGW [66]	<u>67.1</u>	21.9	55.2	33.9	<u>68.6</u>	55.6	50.4	65.1	<u>78.7</u>	88.7	79.9	78.1
MoCo [67]	60.3	19.0	46.6	39.9	57.9	50.7	45.7	64.1	79.8	89.6	79.6	78.3
MoDo [68]	67.9	22.0	55.4	36.0	69.4	<u>56.3</u>	<u>51.2</u>	<u>66.2</u>	78.2	89.8	<u>80.3</u>	<u>78.7</u>
UOWQ	68.2	22.7	56.5	<u>37.2</u>	70.0	57.2	51.9	69.3	77.3	89.5	80.4	79.1

TABLE IV: Training time comparison on the DomainNet dataset across different target domains.

Method	Backbone	DomainNet						
		→C	→I	→P	→Q	→R	→S	Avg
MADA	ViT-S	15:57:00	20:01:00	17:23:30	24:07:30	11:15:00	14:03:30	17:07:55
AllSources \cup Target	ViT-S	10:34:30	10:40:00	10:11:00	08:35:00	08:37:30	10:23:00	09:50:10
UOWQ	ViT-S	10:40:54	10:50:00	10:19:50	08:48:18	08:52:36	10:31:38	10:00:32

TABLE V: Comparison between static and dynamic weighting strategies under the 10-shot setting on the Office-Home dataset.

Method	Backbone	Office-Home				
		→Ar	→Cl	→Pr	→Rw	Avg
<i>Supervised-10-shots:</i>						
Static	ViT-S	74.8	63.1	81.6	83.2	75.7
Dynamic	ViT-S	78.7	65.1	86.9	87.6	79.6

TABLE VI: Multi-Source Transfer with LoRA on Office-Home. We apply LoRA on ViT-B backbone for PEFT.

Method	Backbone	Office-Home				
		→Ar	→Cl	→Pr	→Rw	Avg
<i>Supervised-10-shots Source-Ablation:</i>						
Target-Only	ViT-B	59.8	42.2	69.5	72.0	60.9
Single-Source-avg	ViT-B	72.2	59.9	82.6	81.0	73.9
Single-Source-best	ViT-B	74.4	61.8	84.9	81.9	75.8
AllSources \cup Target	ViT-B	<u>81.1</u>	66.0	88.0	89.2	81.1
OTQMS	ViT-B	81.5	68.0	89.2	90.3	82.3
UOWQ	ViT-B	81.5	<u>67.6</u>	90.1	<u>90.2</u>	82.4

by 0.7 percentage points. Similarly, on *Office-Home*, UOWQ achieves the best average accuracy of 79.1%, surpassing MoDo (78.7%) and MoCo (78.3%) by 0.4 and 0.8 percentage points, respectively.

Consistent and Balanced Multi-Task Performance.

Across the ten target domains from the two benchmarks, UOWQ achieves performance improvements on eight domains compared with the strongest competing methods, demonstrating broad effectiveness across heterogeneous tasks. In particular, the gains are consistent on *DomainNet*, where UOWQ outperforms all baselines across all six target domains (C, I, P, Q, R, and S), indicating that the improvements are not driven by a small subset of tasks. On *Office-Home*, while the improvements are more selective, UOWQ still attains the best overall average accuracy and achieves clear gains on two of the four target domains (Ar and Rw), while remaining competitive on the others. Importantly, improvements on more challenging domains do not come at the expense of degraded performance on easier ones, suggesting effective mitigation of negative task interference. Overall, these results highlight the ability of the proposed method to balance shared representation learning with task-specific optimization in multi-task settings.

Extension of Weighting Theory to Multi-Task Learning.

Although the proposed weighting theory is derived under a multi-source transfer learning formulation, our experiments demonstrate that it generalizes effectively to the multi-task learning setting. This observation validates the effectiveness and generality of the weights introduced by UOWQ. Specifically, UOWQ iteratively optimizes all model parameters and adaptively regulates cross-task influence through weights derived from our theoretical analysis and explicitly related to the transfer quantities.

E. Robustness under Different Shot Settings

We further investigate the robustness of UOWQ with respect to the availability of target samples by gradually increasing the number of shots per class from 5 to 100. Fig. 4 reports the results on the *Office-Home* dataset across all four target domains (Ar, CI, Pr, and Rw), in comparison with Target-Only and AllSources \cup Target. Across all domains, UOWQ maintains consistently competitive accuracy throughout the entire range of shot settings, exhibiting neither performance collapse in low-shot regimes nor degradation as more target samples are introduced. In contrast to methods that rely heavily on either source aggregation or target-only supervision, UOWQ exhibits stable and monotonic performance trends as the number of shots increases. These observations indicate that the proposed approach adapts smoothly to different data regimes and remains robust under varying levels of target supervision.

F. Weight Visualization

To analyze the domain preference learned by UOWQ, we visualize the optimal coefficients α^* (as defined in (23)) together with the base weights w^* (as defined in (25)) in Fig. 5, where each row corresponds to a target domain and each column corresponds to a source domain. On *DomainNet*, when

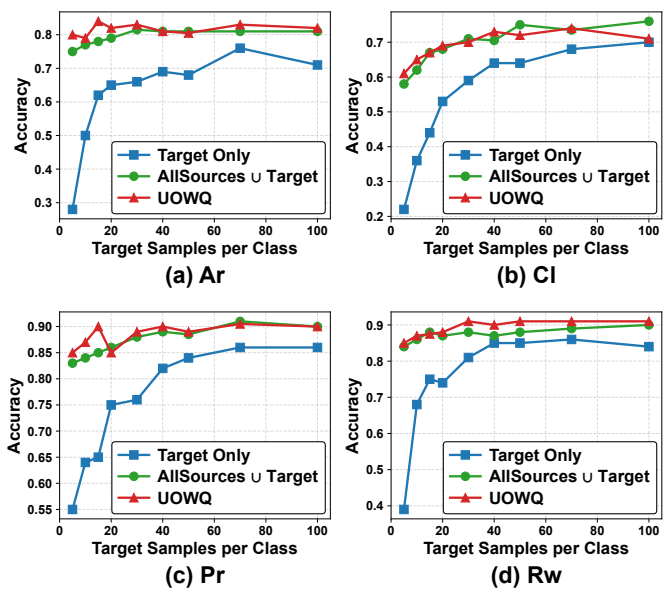


Fig. 4: Performance comparison on the *Office-Home* dataset under varying target shot settings.

Clipart and Painting are treated as target domains, the Real domain receives the largest α^* and w^* coefficients. In addition, the Quickdraw domain receives relatively small weights for any target domain. These observed domain correlations are consistent with previous findings reported in [58]. In *Office-Home*, the Real-World domain obtains the highest α^* for Art, Clipart, and Product targets, which is consistent with previous empirical observations in [69]. Overall, these results suggest that the quadratic optimization naturally assigns larger transfer coefficients to empirically more transferable source domains.

Moreover, Fig. 6 visualizes the learned domain preferences when only half of the source samples are used. Compared with Fig. 5, the relative patterns of the normalized coefficients α remain largely unchanged, indicating that the inferred domain similarity is stable. In contrast, the absolute source weights w become noticeably larger across most source–target pairs. This behavior is consistent with our theory: when the source sample size N_i is reduced, the source effect weakens, and the optimal solution compensates by assigning larger source weights to maintain a favorable bias–variance trade-off. From the (25), since $w_i^* = \frac{s^* \alpha_i^*}{N_i}$ explicitly depends on N_i , decreasing N_i naturally leads to increased w_i . Overall, the comparison between Fig. 5 and Fig. 6 shows that UOWQ adaptively adjusts source weights according to transfer quantities rather than relying on fixed weighting schemes.

G. Computational Efficiency.

We further compare the computational cost of different methods on the *DomainNet* benchmark, and report the wall-clock training time in Table IV. Compared with MADA, which requires substantially longer training time across all target domains, both AllSources \cup Target and UOWQ exhibit significantly improved efficiency. Notably, UOWQ achieves comparable training time to AllSources \cup Target, with only

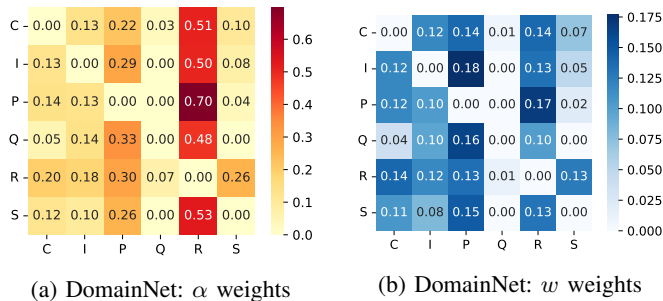
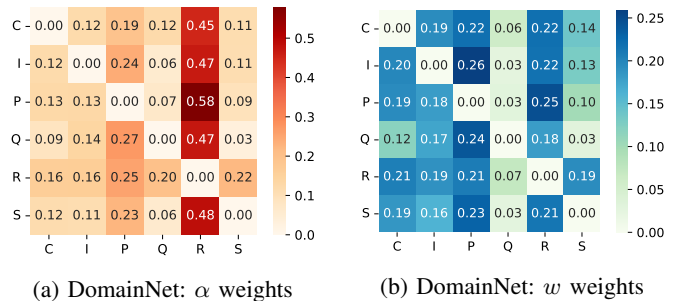
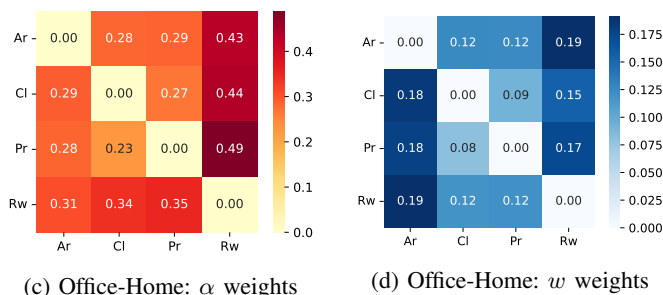
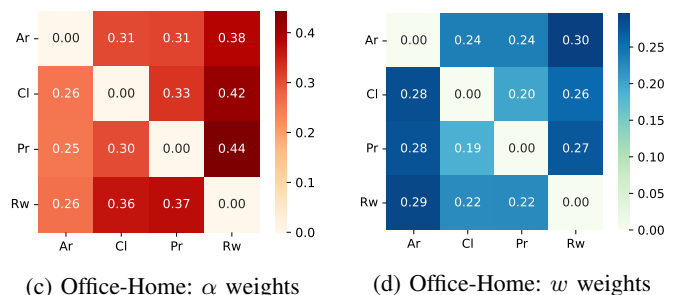
(a) DomainNet: α weights(b) DomainNet: w weights(a) DomainNet: α weights(b) DomainNet: w weights(c) Office-Home: α weights(d) Office-Home: w weights(c) Office-Home: α weights(d) Office-Home: w weights

Fig. 5: Domain preference visualization on DomainNet and Office-Home.

Fig. 6: Domain preference visualization on DomainNet and Office-Home trained with half of the source dataset.

a marginal overhead introduced by the additional optimization procedure. Across all domains, the average training time of UOWQ (10:00:32) remains close to that of AllSources \cup Target (09:50:10), and is substantially lower than MADA (17:07:55). These results indicate that the proposed method introduces minimal computational overhead while providing consistent performance gains, demonstrating a favorable trade-off between effectiveness and efficiency.

H. Static vs. Dynamic Weighting.

Table V further examines the effect of dynamically updating source weights during training. Compared with the static variant, which fixes the weights computed at initialization, the dynamic strategy consistently achieves higher accuracy across all Office-Home target domains. The performance gap is particularly pronounced on more challenging domains such as Clipart and Product, indicating that continuously adapting the weights to the evolving target model is beneficial. These results suggest that dynamic re-optimization enables the transfer strategy to better track changes in the target representation, thereby suppressing suboptimal or outdated source contributions and improving overall robustness under limited target supervision.

I. Compatibility to LoRA-Based Training

We further examine the compatibility of UOWQ with LoRA. Specifically, we apply UOWQ to multi-source transfer on the **Office-Home** dataset using the ViT-B backbone. Each domain is treated as a distinct source task, and LoRA modules with rank 8 are inserted into the projection layers of transformer blocks. As summarized in Table VI, UOWQ consistently improves accuracy over baselines, confirming that the proposed theoretical principles remain effective under LoRA-based adaptation.

VII. CONCLUSION

In this work, we propose UOWQ, a theoretical framework for the unified optimization of source weights and transfer quantities in multi-source transfer learning. By formulating the training process as a parameter estimation problem and conducting an asymptotic analysis of a K-L generalization error measure, we derive a principled method for computing the optimal source weights and transfer quantities. A notable theoretical insight is that, when the source weights are jointly optimized, the optimal strategy is to use all available source samples. This is because enlarging the transfer quantities reduces estimation variance, while adaptive weighting suppresses the bias caused by heterogeneous domains. Building on these theoretical results, we further develop practical algorithms that assign source weights and update them dynamically during training for both multi-source transfer learning and multi-task learning scenarios. Extensive experiments on real-world datasets demonstrate that UOWQ consistently improves performance over state-of-the-art baselines, particularly in few-shot and cross-domain settings. These results validate both the theoretical foundations and the practical advantages of our approach.

REFERENCES

- [1] Q. Xiao, Y. Zhang, and Q. Yang, "Selective random walk for transfer learning in heterogeneous label spaces," *IEEE Transactions on Pattern Analysis and Machine Intelligence*, vol. 46, no. 6, pp. 4476–4488, 2024.
- [2] Z. Zhu, K. Lin, A. K. Jain, and J. Zhou, "Transfer learning in deep reinforcement learning: A survey," *IEEE Transactions on Pattern Analysis and Machine Intelligence*, vol. 45, no. 11, pp. 13 344–13 362, 2023.
- [3] S. Serte, A. Serener, and F. Al-Turjman, "Deep learning in medical imaging: A brief review," *Transactions on Emerging Telecommunications Technologies*, vol. 33, no. 10, p. e4080, 2022.

- [4] J. Devlin, M.-W. Chang, K. Lee, and K. Toutanova, "Bert: Pre-training of deep bidirectional transformers for language understanding," in *Proceedings of the 2019 conference of the North American chapter of the association for computational linguistics: human language technologies, volume 1 (long and short papers)*, 2019, pp. 4171–4186.
- [5] J. Lee, P. Sattigeri, and G. Wornell, "Learning new tricks from old dogs: Multi-source transfer learning from pre-trained networks," *Advances in neural information processing systems*, vol. 32, 2019.
- [6] C. Nguyen, T. Hassner, M. Seeger, and C. Archambeau, "Leep: A new measure to evaluate transferability of learned representations," *International Conference on Machine Learning (ICML)*, 2020.
- [7] X. Tong, X. Xu, S.-L. Huang, and L. Zheng, "A mathematical framework for quantifying transferability in multi-source transfer learning," *Advances in Neural Information Processing Systems*, vol. 34, pp. 26 103–26 116, 2021.
- [8] Z. Han, Z. Zhang, F. Wang, R. He, W. Su, X. Xi, and Y. Yin, "Discriminability and transferability estimation: a bayesian source importance estimation approach for multi-source-free domain adaptation," in *Proceedings of the AAAI conference on artificial intelligence*, vol. 37, no. 6, 2023, pp. 7811–7820.
- [9] Y. Wu, J. Wang, W. Wang, and Y. Li, "H-ensemble: An information theoretic approach to reliable few-shot multi-source-free transfer," in *Proceedings of the AAAI Conference on Artificial Intelligence*, vol. 38, no. 14, 2024, pp. 15 970–15 978.
- [10] D. Li, Z. Zhang, L. Wang, and H. R. Zhang, "Scalable fine-tuning from multiple data sources: A first-order approximation approach," *Findings of the Association for Computational Linguistics: EMNLP 2024*, 2024.
- [11] S. Jain, H. Salman, A. Khaddaj, E. Wong, S. M. Park, and A. Madry, "A data-based perspective on transfer learning," in *Proceedings of the IEEE/CVF Conference on Computer Vision and Pattern Recognition*, 2023, pp. 3613–3622.
- [12] Q. Zhang, H. Fu, G. Huang, Y. Liang, C. Chu, T. Peng, Y. Wu, Q. Li, Y. Li, and S.-L. Huang, "A high-dimensional statistical method for optimizing transfer quantities in multi-source transfer learning," in *The Thirty-ninth Annual Conference on Neural Information Processing Systems*, 2025. [Online]. Available: <https://openreview.net/forum?id=fsTj0BNxyH>
- [13] Z. Wang, Z. Dai, B. Póczos, and J. Carbonell, "Characterizing and avoiding negative transfer," in *Proceedings of the IEEE/CVF conference on computer vision and pattern recognition*, 2019, pp. 11 293–11 302.
- [14] C. Shui, Z. Li, J. Li, C. Gagné, C. X. Ling, and B. Wang, "Aggregating from multiple target-shifted sources," in *International Conference on Machine Learning*. PMLR, 2021, pp. 9638–9648.
- [15] Q. Zhang, C. Chu, H. Fu, T. Peng, and S. Huang, "Asymptotic analysis for optimal source weights in multi-source transfer learning," in *Proceedings of APWDSIT 2025*, 2025.
- [16] B. Liu, Y. Wei, Y. Zhang, and Q. Yang, "Task weighting in multi-task learning via gradient balancing," *NeurIPS*, 2021.
- [17] X. Wang, J. Li, L. Jin, J. Pang, and D. Luo, "Multi-source domain adaptation with mixture of experts," *ECCV*, 2020.
- [18] W. Zhou, H. Wen, and Y. Zhang, "Deep multi-source transfer learning for cross-domain recommendations," *IEEE TKDE*, 2021.
- [19] F. Zhuang, Z. Qi, K. Duan, D. Xi, Y. Zhu, H. Zhu, H. Xiong, and Q. He, "A comprehensive survey on transfer learning," *Proceedings of the IEEE*, vol. 109, no. 1, pp. 43–76, 2020.
- [20] L. Wan, R. Liu, L. Sun, H. Nie, and X. Wang, "Uav swarm based radar signal sorting via multi-source data fusion: A deep transfer learning framework," *Information Fusion*, vol. 78, pp. 90–101, 2022.
- [21] W. Zhang, Z. Lv, H. Zhou, J.-W. Liu, J. Li, M. Li, Y. Li, D. Zhang, Y. Zhuang, and S. Tang, "Revisiting the domain shift and sample uncertainty in multi-source active domain transfer," in *Proceedings of the IEEE/CVF Conference on Computer Vision and Pattern Recognition*, 2024, pp. 16 751–16 761.
- [22] Y. Li, L. Yuan, Y. Chen, P. Wang, and N. Vasconcelos, "Dynamic transfer for multi-source domain adaptation," in *Proceedings of the IEEE/CVF Conference on Computer Vision and Pattern Recognition*, 2021, pp. 10 998–11 007.
- [23] S. Zhao, H. Chen, H. Huang, P. Xu, and G. Ding, "More is better: Deep domain adaptation with multiple sources," *arXiv preprint arXiv:2405.00749*, 2024.
- [24] K. Li, J. Lu, H. Zuo, and G. Zhang, "Multi-source contribution learning for domain adaptation," *IEEE Transactions on Neural Networks and Learning Systems*, vol. 33, no. 10, pp. 5293–5307, 2021.
- [25] S. Zhao, B. Li, P. Xu, X. Yue, G. Ding, and K. Keutzer, "Madan: Multi-source adversarial domain aggregation network for domain adaptation," *International Journal of Computer Vision*, vol. 129, no. 8, pp. 2399–2424, 2021.
- [26] H. Guo, R. Pasunuru, and M. Bansal, "Multi-source domain adaptation for text classification via distancenet-bandits," in *Proceedings of the AAAI conference on artificial intelligence*, vol. 34, no. 05, 2020, pp. 7830–7838.
- [27] R. Caruana, "Multitask learning," *Machine learning*, vol. 28, no. 1, pp. 41–75, 1997.
- [28] A. Kendall, Y. Gal, and R. Cipolla, "Multi-task learning using uncertainty to weigh losses for scene geometry and semantics," in *Proceedings of the IEEE Conference on Computer Vision and Pattern Recognition (CVPR)*, 2018. [Online]. Available: <https://arxiv.org/abs/1705.07115>
- [29] Z. Chen, V. Badrinarayanan, C.-Y. Lee, and A. Rabinovich, "Gradnorm: Gradient normalization for adaptive loss balancing in deep multitask networks," in *International Conference on Machine Learning (ICML)*, 2018. [Online]. Available: <https://arxiv.org/abs/1711.02257>
- [30] S. Liu, E. Johns, and A. J. Davison, "End-to-end multi-task learning with attention," in *Proceedings of the IEEE Conference on Computer Vision and Pattern Recognition (CVPR)*, 2019. [Online]. Available: <https://arxiv.org/abs/1803.10704>
- [31] O. Sener and V. Koltun, "Multi-task learning as multi-objective optimization," in *Advances in Neural Information Processing Systems (NeurIPS)*, 2018. [Online]. Available: <https://arxiv.org/abs/1810.04650>
- [32] X. Zheng, Y. Liu, Y. Hua, Y. Tian, and T. Zhang, "Libra: Balancing tasks for multi-task learning," in *International Conference on Machine Learning (ICML)*, 2021. [Online]. Available: <https://arxiv.org/abs/2107.07018>
- [33] B. Liu, X. Liu, X. Jin, P. Stone, and Q. Liu, "Conflict-averse gradient descent for multi-task learning," in *Advances in Neural Information Processing Systems (NeurIPS)*, 2021. [Online]. Available: <https://arxiv.org/abs/2010.14030>
- [34] Q. Sun, Y. Liu, T.-S. Chua, and B. Schiele, "Adaptive task sampling for meta-learning," in *Advances in Neural Information Processing Systems (NeurIPS)*, 2020. [Online]. Available: <https://arxiv.org/abs/2006.15586>
- [35] K.-K. Maninis, I. Radosavovic, and I. Kokkinos, "Rotograd: Gradient homogenization in multitask learning," in *International Conference on Learning Representations (ICLR)*, 2022, notable Top 5% Paper. [Online]. Available: <https://arxiv.org/abs/2103.14010>
- [36] Y. Du, J. Lin, and P. Zhou, "Game-theoretic optimization for multi-task learning," in *Advances in Neural Information Processing Systems (NeurIPS)*, 2023. [Online]. Available: <https://arxiv.org/abs/2302.02842>
- [37] T. Chen, Y. Sun, and W. Yin, "Flix: A simple and communication-efficient alternative to local methods in federated learning," in *International Conference on Machine Learning (ICML)*, 2023. [Online]. Available: <https://arxiv.org/abs/2302.02842>
- [38] E. Triantafillou, T. Zhu, V. Dumoulin, P. Lamblin, U. Evci, K. Xu, R. Goroshin, C. Gelada, K. Swersky, P.-A. Manzagol *et al.*, "Meta-dataset: A dataset of datasets for learning to learn from few examples," in *International Conference on Learning Representations (ICLR)*, 2020. [Online]. Available: <https://arxiv.org/abs/1903.03096>
- [39] Y. Mansour, M. Mohri, and A. Rostamizadeh, "Domain adaptation with multiple sources," *Advances in neural information processing systems*, vol. 21, 2008.
- [40] M. Long, Y. Cao, J. Wang, and M. Jordan, "Learning transferable features with deep adaptation networks," in *International conference on machine learning*. PMLR, 2015, pp. 97–105.
- [41] H. Zhao, S. Zhang, G. Wu, J. M. Moura, J. P. Costeira, and G. J. Gordon, "Adversarial multiple source domain adaptation," *Advances in neural information processing systems*, vol. 31, 2018.
- [42] Y. Chen, W. Li, C. Sakaridis, D. Dai, and L. Van Gool, "Domain adaptive faster r-cnn for object detection in the wild," in *Proceedings of the IEEE conference on computer vision and pattern recognition*, 2018, pp. 3339–3348.
- [43] M. Long, J. Wang, G. Ding, J. Sun, and P. S. Yu, "Transfer joint matching for unsupervised domain adaptation," in *Proceedings of the IEEE conference on computer vision and pattern recognition*, 2014, pp. 1410–1417.
- [44] N. Courty, R. Flamary, D. Tuia, and A. Rakotomamonjy, "Optimal transport for domain adaptation," *IEEE transactions on pattern analysis and machine intelligence*, vol. 39, no. 9, pp. 1853–1865, 2016.
- [45] X. Chen, S. Wang, J. Wang, and Y. Huang, "Otce: Optimal transport for conditional entropy in transfer learning," *NeurIPS*, 2022.
- [46] K. You, Y. Liu, J. Wang, and M. Long, "Logme: Practical assessment of pre-trained models for transfer learning," *International Conference on Machine Learning (ICML)*, 2021.

- [47] C. Tan, F. Sun, T. Kong, W. Zhang, C. Yang, and C. Liu, "A survey on deep transfer learning," *Neural Networks*, vol. 121, pp. 135–151, 2020.
- [48] H. Liu, M. Long, J. Wang, and Y. Wang, "Geometric-based domain adaptation for transfer learning," *AAAI Conference on Artificial Intelligence*, 2021.
- [49] P. Harremoës and I. Vajda, "On pairs of f -divergences and their joint range," *IEEE Transactions on Information Theory*, vol. 57, no. 6, pp. 3230–3235, 2011.
- [50] Y. Bu, S. Zou, and V. V. Veeravalli, "Tightening mutual information-based bounds on generalization error," *IEEE Journal on Selected Areas in Information Theory*, vol. 1, no. 1, pp. 121–130, 2020.
- [51] T. M. Cover, *Elements of information theory*. John Wiley & Sons, 1999.
- [52] A. W. Van der Vaart, *Asymptotic statistics*. Cambridge university press, 2000, vol. 3.
- [53] M. Raghu, C. Zhang, J. Kleinberg, and S. Bengio, "Transfusion: Understanding transfer learning for medical imaging," *Advances in neural information processing systems*, vol. 32, 2019.
- [54] W. Zhang, L. Deng, L. Zhang, and D. Wu, "A survey on negative transfer," *IEEE/CAA Journal of Automatica Sinica*, vol. 10, no. 2, pp. 305–329, 2022.
- [55] J. Martens, "New insights and perspectives on the natural gradient method," *Journal of Machine Learning Research*, vol. 21, no. 146, pp. 1–76, 2020.
- [56] K. Osawa, S. Li, and T. Hoefler, "Pipefisher: Efficient training of large language models using pipelining and fisher information matrices," *Proceedings of Machine Learning and Systems*, vol. 5, pp. 708–727, 2023.
- [57] H. Venkateswara, J. Eusebio, S. Chakraborty, and S. Panchanathan, "Deep hashing network for unsupervised domain adaptation," in *Proceedings of the IEEE conference on computer vision and pattern recognition*, 2017, pp. 5018–5027.
- [58] X. Peng, Q. Bai, X. Xia, Z. Huang, K. Saenko, and B. Wang, "Moment matching for multi-source domain adaptation," in *Proceedings of the IEEE/CVF international conference on computer vision*, 2019, pp. 1406–1415.
- [59] R. Wightman, "Pytorch image models," <https://github.com/huggingface/pytorch-image-models>, 2019.
- [60] J. Deng, W. Dong, R. Socher, L.-J. Li, K. Li, and L. Fei-Fei, "Imagenet: A large-scale hierarchical image database," in *2009 IEEE conference on computer vision and pattern recognition*. Ieee, 2009, pp. 248–255.
- [61] D. P. Kingma and J. Ba, "Adam: A method for stochastic optimization," *arXiv preprint arXiv:1412.6980*, 2014.
- [62] K. He, X. Zhang, S. Ren, and J. Sun, "Deep residual learning for image recognition," in *Proceedings of the IEEE conference on computer vision and pattern recognition*, 2016, pp. 770–778.
- [63] A. Krizhevsky, I. Sutskever, and G. E. Hinton, "Imagenet classification with deep convolutional neural networks," *Advances in neural information processing systems*, vol. 25, 2012.
- [64] M. Shen, Y. Bu, and G. W. Wornell, "On balancing bias and variance in unsupervised multi-source-free domain adaptation," in *International Conference on Machine Learning*. PMLR, 2023, pp. 30976–30991.
- [65] T. Yu, S. Kumar, A. Gupta, S. Levine, K. Hausman, and C. Finn, "Gradient surgery for multi-task learning," in *International Conference on Learning Representations (ICLR)*, 2020. [Online]. Available: <https://arxiv.org/abs/2001.06782>
- [66] B. Lin, F. Ye, Y. Zhang, and I. Tsang, "Reasonable effectiveness of random weighting: A litmus test for multi-task learning," *Transactions on Machine Learning Research*, 2022.
- [67] H. Fernando, H. Shen, M. Liu, S. Chaudhury, K. Murugesan, and T. Chen, "Mitigating gradient bias in multi-objective learning: A provably convergent stochastic approach," in *ICLR*, 2023.
- [68] L. Chen, H. Fernando, Y. Ying, and T. Chen, "Three-way trade-off in multi-objective learning: Optimization, generalization and conflict-avoidance," *Advances in Neural Information Processing Systems*, vol. 36, pp. 70045–70093, 2023.
- [69] J. Liang, D. Hu, and J. Feng, "Do we really need to access the source data? source hypothesis transfer for unsupervised domain adaptation," in *International conference on machine learning*. PMLR, 2020, pp. 6028–6039.



Qingyue Zhang (Student Member, IEEE) is currently pursuing the Ph.D. degree with the Tsinghua Shenzhen International Graduate School, Tsinghua University, Shenzhen, China. His current research interests include transfer learning and LLM.



Chang Chu (Student Member, IEEE) is currently pursuing the M.S. degree with the Tsinghua Shenzhen International Graduate School, Tsinghua University, Shenzhen, China. His current research interests include transfer learning and class imbalance.



Haohao Fu (Student Member, IEEE) is currently pursuing the Ph.D. degree with the Tsinghua Shenzhen International Graduate School, Tsinghua University, Shenzhen, China. His current research interests include information theory and machine learning.



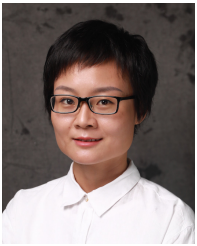
Tianren Peng (Student Member, IEEE) is currently pursuing the Ph.D. degree with the Tsinghua Shenzhen International Graduate School, Tsinghua University, Shenzhen, China. His research interests include machine learning theory and its application in multi-modal learning and transfer learning.



Yanru Wu is currently pursuing the Ph.D. degree with the Tsinghua Shenzhen International Graduate School, Tsinghua University, Shenzhen, China. Her current research interests include transfer learning and continual learning.



Guanbo Huang is currently pursuing the M.S. degree with the Tsinghua Shenzhen International Graduate School, Tsinghua University, Shenzhen, China. His research interests include transfer learning, AIGC, RL, MLLM and Agent application.



Yang Li (Member, IEEE) is an Associate Professor with the School of Artificial Intelligence, The Chinese University of Hong Kong, Shenzhen. Prior to joining CUHK-Shenzhen, she was a postdoctoral researcher at the Tsinghua-Berkeley Shenzhen Institute and later worked with the Institute of Data and Information, Tsinghua Shenzhen International Graduate School. She received the B.A. degree in computer science and mathematics from the Smith College, Northampton, MA, USA, in 2011, and the Ph.D. degree in computer science from Stanford

University, Stanford, CA, USA, in 2017. Her research interests include transfer learning, domain generalization, and interpretable representation learning, with applications to medical image analysis and spatio-temporal data modeling.



Shao-Lun Huang (Member, IEEE) received the B.S. degree (Hons.) from the Department of Electronic Engineering, National Taiwan University, Taipei, Taiwan, in 2008, and the M.S. and Ph.D. degrees from the Department of Electronic Engineering and Computer Sciences, Massachusetts Institute of Technology, Cambridge, MA, USA, in 2010 and 2013, respectively. From 2013 to 2016, he was a Post-Doctoral Researcher with the Department of Electrical Engineering, National Taiwan University, and also with the Department of Electrical Engineering

and Computer Science, Massachusetts Institute of Technology. Since 2016, he has been with the Tsinghua-Berkeley Shenzhen Institute and Tsinghua Shenzhen International Graduate School, Tsinghua University, China, where he is currently an Associate Professor. His current research interests include information theory, communication theory, machine learning, and social networks.

APPENDIX A
JUSTIFICATION OF THE KL-BASED MEASURE

Compared to other measures, the K-L divergence exhibits a closer correspondence with the generalization error as measured by the cross-entropy loss. In this section, we will provide a concrete example (i.e., in a classification task) where the proposed K-L divergence formulation measure aligns with the cross-entropy generalization error.

In a classification task, let $z \in \mathcal{Z}$ denote the input features and $y \in \mathcal{Y}$ represent the output labels. The true data-generating distribution is $P(z, y)$, while the joint distribution model learned from the training dataset is denoted as $\hat{P}_{\hat{\theta}}(z, y)$, where $\hat{\theta}$ denotes the learnable model parameters in training. The proposed measure $D(P \parallel \hat{P})$ is defined as follows.

$$\begin{aligned} D(P \parallel \hat{P}) &= \sum_{z \in \mathcal{Z}, y \in \mathcal{Y}} P(z, y) \log \frac{P(z, y)}{\hat{P}_{\hat{\theta}}(z, y)} \\ &= \sum_{z \in \mathcal{Z}, y \in \mathcal{Y}} P(z, y) \log P(z, y) - \sum_{z \in \mathcal{Z}, y \in \mathcal{Y}} P(z, y) \log \hat{P}_{\hat{\theta}}(y | z) \\ &\quad - \sum_{z \in \mathcal{Z}, y \in \mathcal{Y}} P(z, y) \log \hat{P}(z), \end{aligned} \quad (26)$$

where the second term of (26), i.e.,

$$- \sum_{z \in \mathcal{Z}, y \in \mathcal{Y}} P(z, y) \log \hat{P}_{\hat{\theta}}(y | z),$$

is the standard definition of generalization error in a classification task. Furthermore, the first term of (26) depends solely on the true data distribution and is constant. Though the third term involves $\hat{P}(z)$, $\hat{P}(z)$ is typically treated as a fixed marginal distribution decided by the training data rather than being learned in the model training. As a result, the third term is usually not parameterized by model parameter $\hat{\theta}$, and thus does not contribute to the optimization objective. In brief, the first term and the third term will not affect our optimization. Therefore, the K-L divergence formulation remains consistent with the standard definition of generalization error.

APPENDIX B
PROOF OF THEOREM 2

Proof.

Lemma 6. *In the asymptotic case, the proposed measure (1) and the mean squared error have the relation as follows.*

$$\begin{aligned} \mathbb{E} \left[D \left(P_{X; \theta_0} \parallel P_{X; \hat{\theta}} \right) \right] &= \frac{1}{2} J(\theta_0) \mathbb{E} \left[\left(\hat{\theta} - \theta_0 \right)^2 \right] + \\ &\quad o \left(\mathbb{E} \left[\left(\hat{\theta} - \theta_0 \right)^2 \right] \right) + o \left(\frac{1}{N_0} \right). \end{aligned} \quad (27)$$

Proof. In this section, for the sake of clarity, we will write $\hat{\theta}$ in its parameterized form $\hat{\theta}(X^{N_0})$ when necessary, and these two forms are mathematically equivalent. By taking Taylor expansion of $D \left(P_{X; \theta_0} \parallel P_{X; \hat{\theta}(X^{N_0})} \right)$ at θ_0 , we can get

$$\begin{aligned} &D \left(P_{X; \theta_0} \parallel P_{X; \hat{\theta}(X^{N_0})} \right) \\ &= - \sum_{x \in X} P_{X; \theta_0}(x) \log \frac{P_{X; \hat{\theta}(X^{N_0})}(x)}{P_{X; \theta_0}(x)} \\ &= - \sum_{x \in X} P_{X; \theta_0}(x) \log \left(1 + \frac{P_{X; \hat{\theta}(X^{N_0})}(x) - P_{X; \theta_0}(x)}{P_{X; \theta_0}(x)} \right) \\ &= - \sum_{x \in X} P_{X; \theta_0}(x) \left(\left(\frac{P_{X; \hat{\theta}(X^{N_0})}(x) - P_{X; \theta_0}(x)}{P_{X; \theta_0}(x)} \right) \right. \\ &\quad \left. - \frac{1}{2} \left(\frac{P_{X; \hat{\theta}(X^{N_0})}(x) - P_{X; \theta_0}(x)}{P_{X; \theta_0}(x)} \right)^2 \right) + o(|\hat{\theta}(X^{N_0}) - \theta_0|^2) \\ &= \frac{1}{2} \sum_{x \in X} \frac{\left(P_{X; \hat{\theta}(X^{N_0})}(x) - P_{X; \theta_0}(x) \right)^2}{P_{X; \theta_0}(x)} + o(|\hat{\theta}(X^{N_0}) - \theta_0|^2) \end{aligned} \quad (28)$$

We denote δ as a small constant, and we can rewrite (1) as

$$\begin{aligned} &\mathbb{E} \left[D \left(P_{X; \theta_0} \parallel P_{X; \hat{\theta}(X^{N_0})} \right) \right] \\ &= \sum_{X^{N_0}} P_{X^n; \theta_0}(X^{N_0}) D \left(P_{X; \theta_0} \parallel P_{X; \hat{\theta}(X^{N_0})} \right) \\ &= \sum_{\{X^{N_0}: |\hat{\theta}(X^{N_0}) - \theta_0| < \delta\}} P_{X^n; \theta_0}(X^{N_0}) \cdot \\ &\quad \left(\frac{1}{2} \sum_{x \in X} \frac{\left(P_{X; \hat{\theta}(X^{N_0})}(x) - P_{X; \theta_0}(x) \right)^2}{P_{X; \theta_0}(x)} + o(|\hat{\theta}(X^{N_0}) - \theta_0|^2) \right) \\ &\quad + \sum_{\{X^{N_0}: |\hat{\theta}(X^{N_0}) - \theta_0| \geq \delta\}} P_{X^n; \theta_0}(X^{N_0}) \cdot D \left(P_{X; \theta_0} \parallel P_{X; \hat{\theta}(X^{N_0})} \right) \\ &= \sum_{\{X^{N_0}: |\hat{\theta}(X^{N_0}) - \theta_0| < \delta\}} P_{X^n; \theta_0}(X^{N_0}) \cdot \\ &\quad \left(\frac{1}{2} \sum_{x \in X} \frac{\left(\frac{\partial P_{X; \theta_0}(x)}{\partial \theta_0} (\hat{\theta}(X^{N_0}) - \theta_0) \right)^2}{P_{X; \theta_0}(x)} + o(|\hat{\theta}(X^{N_0}) - \theta_0|^2) \right) \\ &\quad + \sum_{\{X^{N_0}: |\hat{\theta}(X^{N_0}) - \theta_0| \geq \delta\}} P_{X^n; \theta_0}(X^{N_0}) \cdot D \left(P_{X; \theta_0} \parallel P_{X; \hat{\theta}(X^{N_0})} \right) \end{aligned} \quad (29)$$

To facilitate the subsequent proof, we introduce the concept of "Dot Equal".

Definition 7. (*Dot Equal* (\doteq)) Specifically, given two functions $f(n)$ and $g(n)$, the notation $f(n) \doteq g(n)$ is defined as

$$f(n) \doteq g(n) \Leftrightarrow \lim_{n \rightarrow \infty} \frac{1}{n} \log \frac{f(n)}{g(n)} = 0, \quad (30)$$

which shows that $f(n)$ and $g(n)$ have the same exponential decaying rate.

We denote $\hat{P}_{X^{N_0}}$ as the empirical distribution of X^{N_0} . Applying Sanov's Theorem to (29), we can know that

$$P_{X^n; \theta_0}(X^{N_0}) \doteq e^{-N_0 D(\hat{P}_{X^{N_0}} \parallel P_{X; \theta_0})} \quad (31)$$

Then, we aim to establish a connection between (31) and $|\hat{\theta}(X^{N_0}) - \theta_0|^2$. From (28), we can know that the $D(\hat{P}_{X^{N_0}} \| P_{X;\theta_0})$ in (31) can be transformed to

$$\begin{aligned} & D(\hat{P}_{X^{N_0}} \| P_{X;\theta_0}) \\ &= \frac{1}{2} \sum_{x \in X} \frac{(\hat{P}_{X^{N_0}}(x) - P_{X;\theta_0}(x))^2}{\hat{P}_{X^{N_0}}(x)} + o(|\hat{\theta}(X^{N_0}) - \theta_0|^2) \\ &= \frac{1}{2} \sum_{x \in X} \frac{(\hat{P}_{X^{N_0}}(x) - P_{X;\theta_0}(x))^2}{P_{X;\theta_0}(x)} + o(|\hat{\theta}(X^{N_0}) - \theta_0|^2) \end{aligned} \quad (32)$$

From the characteristics of MLE, we can know that

$$\begin{aligned} & \mathbb{E}_{\hat{P}_{X^{N_0}}} \left[\frac{\partial \log P_{X;\hat{\theta}(X^{N_0})}(x)}{\partial \hat{\theta}} \right] \\ &= 0 \\ &= \mathbb{E}_{\hat{P}_{X^{N_0}}} \left[\frac{\partial \log P_{X;\theta_0}(x)}{\partial \theta_0} \right] \\ &+ \mathbb{E}_{\hat{P}_{X^{N_0}}} \left[\frac{\partial^2 \log P_{X;\theta_0}(x)}{\partial \theta_0^2} \right] (\hat{\theta}(X^{N_0}) - \theta_0) \\ &+ O(|\hat{\theta}(X^{N_0}) - \theta_0|^2), \end{aligned} \quad (33)$$

which can be transformed to

$$\begin{aligned} & (\hat{\theta}(X^{N_0}) - \theta_0) + O(|\hat{\theta}(X^{N_0}) - \theta_0|^2) \\ &= - \frac{\mathbb{E}_{\hat{P}_{X^{N_0}}} \left[\frac{\partial \log P_{X;\theta_0}(x)}{\partial \theta_0} \right]}{\mathbb{E}_{\hat{P}_{X^{N_0}}} \left[\frac{\partial^2 \log P_{X;\theta_0}(x)}{\partial \theta_0^2} \right]} \\ &= - \frac{\mathbb{E}_{\hat{P}_{X^{N_0}}} \left[\frac{\frac{\partial P_{X;\theta_0}(x)}{\partial \theta_0}}{P_{X;\theta_0}(x)} \right]}{\mathbb{E}_{\hat{P}_{X^{N_0}}} \left[\frac{\partial^2 \log P_{X;\theta_0}(x)}{\partial \theta_0^2} \right]} \\ &= \frac{\sum_{x \in \mathcal{X}} (\hat{P}_{X^{N_0}}(x) - P_{X;\theta_0}(x)) \frac{\frac{\partial P_{X;\theta_0}(x)}{\partial \theta_0}}{P_{X;\theta_0}(x)}}{J(\theta_0)} \end{aligned} \quad (34)$$

Using the Cauchy-Schwarz inequality, we can obtain

$$\begin{aligned} & \sum_{x \in X} \frac{(\hat{P}_{X^{N_0}}(x) - P_{X;\theta_0}(x))^2}{P_{X;\theta_0}(x)} \cdot \sum_x \frac{(\frac{\partial P_{X;\theta_0}(x)}{\partial \theta_0})^2}{P_{X;\theta_0}(x)} \geq \\ & \left(\sum_{x \in X} (\hat{P}_{X^{N_0}}(x) - P_{X;\theta_0}(x)) \frac{\frac{\partial P_{X;\theta_0}(x)}{\partial \theta_0}}{P_{X;\theta_0}(x)} \right)^2 \end{aligned} \quad (35)$$

where

$$\begin{aligned} & \sum_x \frac{(\frac{\partial P_{X;\theta_0}(x)}{\partial \theta_0})^2}{P_{X;\theta_0}(x)} = \sum_x P_{X;\theta_0}(x) \left(\frac{1}{P_{X;\theta_0}(x)} \frac{\partial P_{X;\theta_0}(x)}{\partial \theta_0} \right)^2 \\ &= \sum_x P_{X;\theta_0}(x) \left(\frac{\partial \log P_{X;\theta_0}(x)}{\partial \theta_0} \right)^2 = J(\theta_0) \end{aligned} \quad (36)$$

Combining with (32), (34), and (36), the inequality (35) can be transformed to

$$\begin{aligned} & D(\hat{P}_{X^{N_0}} \| P_{X;\theta_0}) \\ &= \frac{1}{2} \sum_{x \in X} \frac{(\hat{P}_{X^{N_0}}(x) - P_{X;\theta_0}(x))^2}{P_{X;\theta_0}(x)} + o(|\hat{\theta}(X^{N_0}) - \theta_0|^2) \\ &\geq \frac{1}{2} J(\theta_0) (\hat{\theta}(X^{N_0}) - \theta_0 + O(|\hat{\theta}(X^{N_0}) - \theta_0|^2))^2 \\ &+ o(|\hat{\theta}(X^{N_0}) - \theta_0|^2) \\ &= \frac{1}{2} J(\theta_0) |\hat{\theta}(X^{N_0}) - \theta_0|^2 + o(|\hat{\theta}(X^{N_0}) - \theta_0|^2) \end{aligned} \quad (37)$$

Combining (31) and (37), we can know that

$$P_{X^{N_0};\theta_0}(X^{N_0}) \doteq e^{-N_0 D(\hat{P}_{X^{N_0}} \| P_{X;\theta_0})} \leq e^{-\frac{N_0 J(\theta_0) |\hat{\theta}(X^{N_0}) - \theta_0|^2}{2}} \quad (38)$$

For the first term in (29), the negligible term $o(|\hat{\theta}(X^{N_0}) - \theta_0|^2)$ is of lower order than the main term and can therefore be ignored. As for the second term in (29), its probability is bounded by $O(e^{-\frac{N_0 J(\theta_0) |\hat{\theta}(X^{N_0}) - \theta_0|^2}{2}})$ according to (38), which decays exponentially with N_0 . Consequently, this probability is $o(1/N_0)$, since exponential decay in N_0 dominates any polynomial rate. Moreover, under the compactness assumption on the parameter space stated in Section III-C, the K-L divergence is uniformly bounded, implying that the entire second term is $o(1/N_0)$. By transferring (29), we can get

$$\begin{aligned} & \mathbb{E} \left[D(P_{X;\theta_0} \| P_{X;\hat{\theta}(X^{N_0})}) \right] \\ &= \frac{1}{2} \mathbb{E} \left[\sum_{x \in X} \frac{\left(\frac{\partial P_{X;\theta_0}(x)}{\partial \theta_0} (\hat{\theta}(X^{N_0}) - \theta_0) \right)^2}{P_{X;\theta_0}(x)} \right] \\ &+ o \left(\mathbb{E} \left[(\hat{\theta} - \theta_0)^2 \right] \right) + o\left(\frac{1}{N_0}\right). \end{aligned} \quad (39)$$

We then transform (39) with (36)

$$\begin{aligned} & \frac{1}{2} \mathbb{E} \left[\sum_{x \in X} \frac{\left(\frac{\partial P_{X;\theta_0}(x)}{\partial \theta_0} (\hat{\theta}(X^{N_0}) - \theta_0) \right)^2}{P_{X;\theta_0}(x)} \right] \\ &= \frac{1}{2} \mathbb{E} \left[(\hat{\theta} - \theta_0)^2 \right] \sum_x \frac{(\frac{\partial P_{X;\theta_0}(x)}{\partial \theta_0})^2}{P_{X;\theta_0}(x)} \\ &= \frac{1}{2} \mathbb{E} \left[(\hat{\theta} - \theta_0)^2 \right] J(\theta_0) \end{aligned} \quad (40)$$

Combining (39), (40), we can get

$$\begin{aligned} \mathbb{E} \left[D(P_{X;\theta_0} \| P_{X;\hat{\theta}}) \right] &= \frac{1}{2} \mathbb{E} \left[(\hat{\theta} - \theta_0)^2 \right] J(\theta_0) + \\ &o \left(\mathbb{E} \left[(\hat{\theta} - \theta_0)^2 \right] \right) + o\left(\frac{1}{N_0}\right). \end{aligned} \quad (41)$$

□

We denote $E_{\hat{\theta}}$ as the expectation of $\hat{\theta}$. Then, we can make a decomposition of the K-L measure, i.e.,

$$\begin{aligned} & \mathbb{E} \left[D \left(P_{X;\theta_0} \middle\| P_{X;\hat{\theta}} \right) \right] \\ &= \frac{1}{2} \mathbb{E} \left[\left(\hat{\theta} - \theta_0 \right)^2 \right] J(\theta_0) + o\left(\frac{1}{N_0}\right) \\ &= \frac{1}{2} J(\theta_0) \left(\mathbb{E} \left[\left(\hat{\theta} - E_{\hat{\theta}} \right)^2 \right] + \mathbb{E} \left[\left(E_{\hat{\theta}} - \theta_0 \right)^2 \right] \right) \\ &+ o \left(\mathbb{E} \left[\left(\hat{\theta} - E_{\hat{\theta}} \right)^2 \right] + \mathbb{E} \left[\left(E_{\hat{\theta}} - \theta_0 \right)^2 \right] \right) + o\left(\frac{1}{N_0}\right). \end{aligned} \quad (42)$$

In the following, we first derive the expression of $E_{\hat{\theta}}$, as well as the distributional expression of $(\hat{\theta} - E_{\hat{\theta}})$. We then use these results to obtain the representation of the K-L measure. In our setting, the MLE and its expected definition are given as follows.

$$\hat{\theta} \triangleq \arg \max_{\theta} L_n(\theta), \quad (43)$$

$$E_{\hat{\theta}} \triangleq \arg \max_{\theta} L(\theta). \quad (44)$$

where

$$L_n(\theta) = \frac{\sum_{x \in X^{N_0}} \log P_{X;\theta}(x) + \sum_{x \in X^{n_1}} w_1 \log P_{X;\theta}(x)}{N_0 + w_1 n_1}, \quad (45)$$

$$L(\theta) = \frac{N_0 \mathbb{E}_{\theta_0} [\log P_{X;\theta}(x)] + w_1 n_1 \mathbb{E}_{\theta_1} [\log P_{X;\theta}(x)]}{N_0 + w_1 n_1}. \quad (46)$$

For $E_{\hat{\theta}}$, we have the following lemma to establish its relation to the θ_0 and θ_1 .

Lemma 8. $E_{\hat{\theta}}$ is a weighted average of θ_0 and θ_1 , given by

$$E_{\hat{\theta}} = \frac{N_0 \theta_0 + w_1 n_1 \theta_1}{N_0 + w_1 n_1} + O\left(\frac{1}{N_0}\right). \quad (47)$$

Proof. We could equivalently transform (44) into

$$E_{\hat{\theta}} \triangleq \arg \min_{\theta} -L(\theta). \quad (48)$$

We then employ the Lagrangian method to solve this minimization problem. We treat $P_{X;\theta}(x), \forall x \in \mathcal{X}$ as the variables with constraint

$$\sum_{x \in \mathcal{X}} P_{X;\theta}(x) = 1. \quad (49)$$

Then we can construct the corresponding Lagrangian function

$$\begin{aligned} \text{Lagrangian}(P, \lambda) &= - \sum_{x \in \mathcal{X}} \left(\frac{N_0 P_{X;\theta_0}(x)}{N_0 + w_1 n_1} + \right. \\ &\left. \frac{w_1 n_1 P_{X;\theta_1}(x)}{N_0 + w_1 n_1} \right) \log P_{X;\theta}(x) + \lambda \left(\sum_{x \in \mathcal{X}} P_{X;\theta}(x) - 1 \right). \end{aligned} \quad (50)$$

By jointly solving the first-order necessary conditions

$$\frac{\partial \text{Lagrangian}(P, \lambda)}{\partial P_{X;\theta}(x)} = 0, \forall x \in \mathcal{X} \quad (51)$$

$$\frac{\partial \text{Lagrangian}(P, \lambda)}{\partial \lambda} = 0, \quad (52)$$

we have

$$P_{X;E_{\hat{\theta}}}(x) = \frac{N_0 P_{X;\theta_0}(x) + w_1 n_1 P_{X;\theta_1}(x)}{N_0 + w_1 n_1}, \forall x \in \mathcal{X}. \quad (53)$$

By doing a Taylor Expansion of (53) around θ_0 , we can get

$$\begin{aligned} & P_{X;\theta_0}(x) + \frac{\partial P_{X;\theta_0}(x)}{\partial \theta} (E_{\hat{\theta}} - \theta_0) + O(|E_{\hat{\theta}} - \theta_0|^2) \\ &= \frac{N_0}{N_0 + w_1 n_1} P_{X;\theta_0}(x) + \frac{w_1 n_1}{N_0 + w_1 n_1} \left(P_{X;\theta_0}(x) + \right. \\ &\left. \frac{\partial P_{X;\theta_0}(x)}{\partial \theta} (\theta_1 - \theta_0) + O(|\theta_0 - \theta_1|^2) \right). \end{aligned} \quad (54)$$

From (54) we can get

$$E_{\hat{\theta}} = \frac{N_0 \theta_0 + w_1 n_1 \theta_1}{N_0 + w_1 n_1} + O(|\theta_0 - \theta_1|^2), \quad (55)$$

So we can get

$$E_{\hat{\theta}} = \frac{N_0 \theta_0 + w_1 n_1 \theta_1}{N_0 + w_1 n_1} + O\left(\frac{1}{N_0}\right). \quad (56)$$

□

Because $\hat{\theta}$ is a maximizer of $L_n(\hat{\theta})$, $E_{\hat{\theta}}$ is a maximizer of $L(\hat{\theta})$, we can get

$$L'_n(\hat{\theta}) = 0 = L'_n(E_{\hat{\theta}}) + L''_n(E_{\hat{\theta}})(\hat{\theta} - E_{\hat{\theta}}), \quad (57)$$

$$\begin{aligned} L'(E_{\hat{\theta}}) = 0 &= \frac{N_0}{N_0 + w_1 n_1} \mathbb{E}_{\theta_0} \left[\frac{\partial \log P_{X;E_{\hat{\theta}}}(x)}{\partial \theta} \right] \\ &+ \frac{w_1 n_1}{N_0 + w_1 n_1} \mathbb{E}_{\theta_1} \left[\frac{\partial \log P_{X;E_{\hat{\theta}}}(x)}{\partial \theta} \right]. \end{aligned} \quad (58)$$

By transforming (57), we have

$$\sqrt{N_0 + w_1 n_1} (\hat{\theta} - E_{\hat{\theta}}) = - \frac{\sqrt{N_0 + w_1 n_1} L'_n(E_{\hat{\theta}})}{L''_n(E_{\hat{\theta}})}. \quad (59)$$

Combining with (58), we can transform the numerator of the right-hand side of (59) as follows:

$$\begin{aligned} & \sqrt{N_0 + w_1 n_1} L'_n(E_{\hat{\theta}}) \\ &= \sqrt{N_0 + w_1 n_1} (L'_n(E_{\hat{\theta}}) - L'(E_{\hat{\theta}})) \\ &= \sqrt{\frac{N_0}{N_0 + w_1 n_1}} \left(\sqrt{\frac{1}{N_0}} \sum_{x \in X^{N_0}} \frac{\partial \log P_{X;E_{\hat{\theta}}}(x)}{\partial \theta} \right. \\ &\quad \left. - \sqrt{N_0} \mathbb{E}_{\theta_0} \left[\frac{\partial \log P_{X;E_{\hat{\theta}}}(x)}{\partial \theta} \right] \right) \\ &+ \sqrt{\frac{w_1 n_1}{N_0 + w_1 n_1}} \left(\sqrt{\frac{1}{w_1 n_1}} \sum_{x \in X^{n_1}} w_1 \frac{\partial \log P_{X;E_{\hat{\theta}}}(x)}{\partial \theta} \right. \\ &\quad \left. - \sqrt{w_1 n_1} \mathbb{E}_{\theta_1} \left[\frac{\partial \log P_{X;E_{\hat{\theta}}}(x)}{\partial \theta} \right] \right). \end{aligned} \quad (60)$$

Applying the Central Limit Theorem to (60), we can get

$$\begin{aligned} & \sqrt{N_0 + w_1 n_1} L'_n(E_{\hat{\theta}}) \xrightarrow{a.s.} \\ & \mathcal{N}\left(0, \frac{N_0}{N_0 + w_1 n_1} \left(\mathbb{E}_{\theta_0} \left[\left(\frac{\partial \log P_{X;E_{\hat{\theta}}}(x)}{\partial \theta} \right)^2 \right] \right. \right. \\ & \quad \left. \left. - \mathbb{E}_{\theta_0} \left[\left(\frac{\partial \log P_{X;E_{\hat{\theta}}}(x)}{\partial \theta} \right) \right]^2 \right) + \right. \\ & \quad \left. \frac{w_1^2 n_1}{N_0 + w_1 n_1} \left(\mathbb{E}_{\theta_1} \left[\left(\frac{\partial \log P_{X;E_{\hat{\theta}}}(x)}{\partial \theta} \right)^2 \right] \right. \right. \\ & \quad \left. \left. - \mathbb{E}_{\theta_1} \left[\left(\frac{\partial \log P_{X;E_{\hat{\theta}}}(x)}{\partial \theta} \right) \right]^2 \right) \right) \end{aligned} \quad (61)$$

By taking Taylor expansion of $E_{\hat{\theta}}$ at θ_0 , we can get

$$\begin{aligned} & \mathbb{E}_{\theta_0} \left[\left(\frac{\partial \log P_{X;E_{\hat{\theta}}}(x)}{\partial \theta} \right)^2 \right] \\ &= \mathbb{E}_{\theta_0} \left[\left(\frac{\partial \log P_{X;\theta_0}(x)}{\partial \theta} + \frac{\partial}{\partial \theta} \frac{\partial \log P_{X;\theta_0}(x)}{\partial \theta} (E_{\hat{\theta}} - \theta_0) \right. \right. \\ & \quad \left. \left. + O\left(\frac{1}{N_0}\right) \right)^2 \right] \\ &= J(\theta_0) + (E_{\hat{\theta}} - \theta_0) \mathbb{E}_{\theta_0} \left[\frac{\partial \log P_{X;E_{\hat{\theta}}}(x)}{\partial \theta} \frac{\partial^2 \log P_{X;E_{\hat{\theta}}}(x)}{\partial \theta^2} \right] \\ & \quad + O\left(\frac{1}{N_0}\right) \\ &= J(\theta_0) + O\left(\frac{1}{\sqrt{N_0}}\right) \end{aligned} \quad (63)$$

and

$$\begin{aligned} & \mathbb{E}_{\theta_0} \left[\left(\frac{\partial \log P_{X;E_{\hat{\theta}}}(x)}{\partial \theta} \right)^2 \right] \\ &= \mathbb{E}_{\theta_0} \left[\left(\frac{\partial \log P_{X;\theta_0}(x)}{\partial \theta} + \frac{\partial}{\partial \theta} \frac{\partial \log P_{X;\theta_0}(x)}{\partial \theta} (E_{\hat{\theta}} - \theta_0) \right. \right. \\ & \quad \left. \left. + O\left(\frac{1}{N_0}\right) \right)^2 \right] \\ &= \mathbb{E}_{\theta_0} \left[\left(\frac{\partial}{\partial \theta} \frac{\partial \log P_{X;\theta_0}(x)}{\partial \theta} (E_{\hat{\theta}} - \theta_0) + O\left(\frac{1}{N_0}\right) \right)^2 \right] \\ &= (E_{\hat{\theta}} - \theta_0)^2 \mathbb{E}_{\theta_0} \left[\left(\frac{\partial}{\partial \theta} \frac{\partial \log P_{X;\theta_0}(x)}{\partial \theta} \right)^2 \right] + o\left(\frac{1}{N_0}\right) \\ &= O\left(\frac{1}{N_0}\right) \end{aligned} \quad (64)$$

Similarly to (63) and (64), we can prove

$$\mathbb{E}_{\theta_1} \left[\left(\frac{\partial \log P_{X;E_{\hat{\theta}}}(x)}{\partial \theta} \right)^2 \right] = J(\theta_1) + O\left(\frac{1}{\sqrt{N_0}}\right), \quad (65)$$

and

$$\mathbb{E}_{\theta_1} \left[\left(\frac{\partial \log P_{X;E_{\hat{\theta}}}(x)}{\partial \theta} \right)^2 \right] = O\left(\frac{1}{N_0}\right). \quad (66)$$

By substituting (63), (64), (65), and (66) into (61), we obtain

$$\begin{aligned} & \sqrt{N_0 + w_1 n_1} L'_n(E_{\hat{\theta}}) \xrightarrow{a.s.} \\ & \mathcal{N}\left(0, \frac{N_0}{N_0 + w_1 n_1} J(\theta_0) + \frac{w_1^2 n_1}{N_0 + w_1 n_1} J(\theta_1)\right). \end{aligned} \quad (67)$$

Moreover, we know $L''_n(E_{\hat{\theta}}) \xrightarrow{P} -J(E_{\hat{\theta}})$. Given that θ_0, θ_1 , and $E_{\hat{\theta}}$ are already assumed to be sufficiently close, we can use this, along with a Taylor expansion, to estimate the distance between their Fisher information matrices. We conclude that the discrepancy among $J(\theta_0)$, $J(\theta_1)$, and $J(E_{\hat{\theta}})$ is of the order $O\left(\frac{1}{\sqrt{N_0}}\right)$.

$$\begin{aligned} J(\theta_1) &= \mathbb{E}_{\theta_1} \left[\left(\frac{\partial}{\partial \theta} \log P_{X;\theta_1} \right)^2 \right] \\ &= \mathbb{E}_{\theta_1} \left[\left(\frac{\partial}{\partial \theta} \log P_{X;\theta_0} + \frac{\partial^2 \log P_{X;\theta_0}}{\partial \theta^2} (\theta_1 - \theta_0) \right. \right. \\ & \quad \left. \left. + O\left(\frac{1}{N_0}\right) \right)^2 \right] \\ &= \mathbb{E}_{\theta_1} \left[\left(\frac{\partial}{\partial \theta} \log P_{X;\theta_0} \right)^2 \right] + O\left(\frac{1}{\sqrt{N_0}}\right) \\ &= \sum_{x \in \mathcal{X}} P_{X;\theta_1}(x) \left(\frac{\partial}{\partial \theta} \log P_{X;\theta_0}(x) \right)^2 + O\left(\frac{1}{\sqrt{N_0}}\right) \\ &= \sum_{x \in \mathcal{X}} \left(P_{X;\theta_0}(x) + \frac{\partial P_{X;\theta_0}}{\partial \theta} (\theta_1 - \theta_0) + O\left(\frac{1}{N_0}\right) \right)^2. \end{aligned} \quad (68)$$

$$\begin{aligned} & \left(\frac{\partial}{\partial \theta} \log P_{X;\theta_0}(x) \right)^2 + O\left(\frac{1}{\sqrt{N_0}}\right) \\ &= \sum_{x \in \mathcal{X}} P_{X;\theta_0}(x) \left(\frac{\partial}{\partial \theta} \log P_{X;\theta_0}(x) \right)^2 + O\left(\frac{1}{\sqrt{N_0}}\right) \end{aligned} \quad (69)$$

$$= J(\theta_0) + O\left(\frac{1}{\sqrt{N_0}}\right) \quad (70)$$

Combining with (59) and (67),

$$(\hat{\theta} - E_{\hat{\theta}}) \xrightarrow{d} N\left(0, \frac{N_0 + w_1^2 n_1}{(N_0 + w_1 n_1)^2} \frac{1}{J(\theta_0)}\right). \quad (71)$$

Substituting (47) and (71) into (42), we have

$$\begin{aligned} & \mathbb{E} \left[D(P_{X;\theta_0} \| P_{X;\hat{\theta}}) \right] \\ &= \frac{1}{2} \frac{N_0 + w_1^2 n_1}{(N_0 + w_1 n_1)^2} + \frac{1}{2} \frac{(w_1 n_1)^2 J(\theta_0) (\theta_0 - \theta_1)^2}{(N_0 + w_1 n_1)^2} + o\left(\frac{1}{N_0}\right). \end{aligned} \quad (72)$$

By differentiating with respect to w_1 , we obtain the optimal value of weight is

$$w_1^* = \frac{1}{1 + t n_1} \quad (73)$$

Similarly, by taking the derivative of (72) with respect to n_1 , we observe that the derivative is

$$-\frac{1}{2} \left(\frac{1 + n_1 t}{N_0 + n_1 + N_0 n_1 t} \right), \quad (74)$$

which is strictly negative, implying that the optimal value of n_1 is N_1 . Finally, we obtain the optimal value of weight in (10). \square

APPENDIX C
PROOF OF PROPOSITION 3

Proof. Similar to (42), we can get

$$\begin{aligned} & \mathbb{E} \left[D \left(P_{X;\underline{\theta}_0} \parallel P_{X;\hat{\theta}} \right) \right] \\ &= \frac{1}{2} \text{tr} \left(J(\underline{\theta}_0) \mathbb{E} \left[\left(\hat{\theta} - E_{\hat{\theta}} \right) \left(\hat{\theta} - E_{\hat{\theta}} \right)^\top \right] \right) \\ &+ \frac{1}{2} \text{tr} \left(J(\underline{\theta}_0) \mathbb{E} \left[\left(E_{\hat{\theta}} - \underline{\theta}_0 \right) \left(E_{\hat{\theta}} - \underline{\theta}_0 \right)^\top \right] \right) + o\left(\frac{1}{N_0}\right). \end{aligned} \quad (75)$$

Similar to (71), we can get

$$\left(\hat{\theta} - E_{\hat{\theta}} \right) \xrightarrow{d} \mathcal{N} \left(0, \frac{N_0 + w_1^2 n_1}{(N_0 + w_1 n_1)^2} J(\underline{\theta}_0)^{-1} \right). \quad (76)$$

So we can know that $\mathbb{E} \left[\left(\hat{\theta} - E_{\hat{\theta}} \right) \left(\hat{\theta} - E_{\hat{\theta}} \right)^\top \right]$ has the limit

$$\frac{N_0 + w_1^2 n_1}{(N_0 + w_1 n_1)^2} J(\underline{\theta}_0)^{-1} \quad (77)$$

The same to Lemma 8, we can get

$$E_{\hat{\theta}} = \frac{N_0 \underline{\theta}_0 + w_1 n_1 \underline{\theta}_1}{N_0 + w_1 n_1} + O\left(\frac{1}{N_0}\right), \quad (78)$$

Combining (75), (76) and (78), we can know that the K-L measure has the form of (11). \square

APPENDIX D
PROOF OF THEOREM 5

Proof. Similar to (71), we can get

$$\left(\hat{\theta} - E_{\hat{\theta}} \right) \xrightarrow{d} \mathcal{N} \left(0, \frac{N_0 + \sum_{i=1}^K w_i^2 n_i}{\left(N_0 + \sum_{i=1}^K w_i n_i \right)^2} J(\underline{\theta}_0)^{-1} \right). \quad (79)$$

Similar to Lemma 8, we can get

$$E_{\hat{\theta}} = \frac{N_0 \underline{\theta}_0 + \sum_{i=1}^k w_i n_i \underline{\theta}_i}{N_0 + s} + O\left(\frac{1}{N_0}\right). \quad (80)$$

Combining (75), (79) and (80), the K-L measure is

$$\frac{d}{2} \left(\frac{N_0 + \sum_{i=1}^K \frac{b_i^2}{n_i}}{(N_0 + s)^2} + \frac{s^2}{(N_0 + s)^2} \frac{\underline{\alpha}^T \Theta^T J(\underline{\theta}_0) \Theta \underline{\alpha}}{d} \right) + o\left(\frac{1}{N_0}\right). \quad (81)$$

According to (5), it is easy to observe that the optimal performance is achieved when every n_i takes its maximum value N_i . Then, we can transform (81) to

$$\begin{aligned} & \frac{d}{2} \left(\frac{N_0}{(N_0 + s)^2} + \frac{s^2}{(N_0 + s)^2} \underline{\alpha}^T \text{diag} \left(\frac{1}{N_1}, \dots, \frac{1}{N_K} \right) \underline{\alpha} \right. \\ & \left. + \frac{s^2}{(N_0 + s)^2} \frac{\underline{\alpha}^T \Theta^T J(\underline{\theta}_0) \Theta \underline{\alpha}}{d} \right) + o\left(\frac{1}{N_0}\right). \end{aligned} \quad (82)$$

\square